Current Research in Biotechnology 4 (2022) 32–46

Contents lists available at ScienceDirect

Current Research in Biotechnology

journal homepage: www.elsevier.com/locate/crbiot

Metabolic engineering of *Corynebacterium glutamicum* for *de novo* production of 3-hydroxycadaverine

Carina Prell [a], Sophie-Ann Vonderbank [a], Florian Meyer [a], Fernando Pérez-García [b], Volker F. Wendisch [a,*]

[a] Genetics of Prokaryotes, Faculty of Biology & CeBiTec, Bielefeld University, Bielefeld, Germany
[b] Department of Biotechnology and Food Science, Norwegian University of Science and Technology, Trondheim, Norway

ARTICLE INFO

Keywords:
Corynebacterium glutamicum
Hydroxylation
Decarboxylation
4-hydroxylysine
3-hydroxycadaverine
Fermentation
Metabolic engineering

ABSTRACT

Functionalization of amino acids and their derivatives opens up the possibility to produce novel compounds with additional functional groups, which can expand their application spectra. Hydroxylation of polyamide building blocks might allow crosslinking between the molecular chains by esterification. Consequently, this can alter the functional properties of the resulting polymers. *C. glutamicum* represents a well-known industrial workhorse and has been used extensively to produce lysine and lysine derivatives. These are used as building blocks for chemical and pharmaceutical applications. In this study, it was shown for the first time that C3-hydroxylated cadaverine can be produced *de novo* by a lysine overproducing *C. glutamicum* strain. The lysine hydroxylase from *Flavobacterium johnsoniae* is highly specific for its natural substrate lysine and, therefore, hydroxylation of lysine precedes decarboxylation of 4-hydroxylysine (4-HL) to 3-hydroxycadaverine (3-HC). For optimal precursor supply, various cultivation parameters were investigated identifying the iron concentration and pH as major effectors on 4-HL production, whereas the supply with the cosubstrate 2-oxoglutarate (2-OG) was sufficient. Deletion of the gene coding for the lysine exporter LysE suggested that the exporter may also be involved in the export of the structurally similar 4-HL. With the optimised setting for 4-HL production, the pathway was extended towards 3-HC by decarboxylation. Three different genes coding for lysine/4-HL decarboxylases, LdcC and CadA from *E. coli* and DC_{Fj} from *F. johnsoniae,* were expressed in the 4-HL producing strain and compared regarding 3-HC production. It was shown in a semi-preparative biocatalysis that all three decarboxylases can accept 4-HL as substrate with varying efficiencies. *In vivo,* LdcC supported 3-HC production best with a final titer of 11 mM. To improve titers a fed-batch cultivation in 1 L bioreactor scale was performed and the plasmid-based overexpression of *ldcC* was induced after 24 h resulting in the highest titer of 8.6 g L^{-1} (74 mM) of 3-hydroxycadaverine reported up to now.

Contents

* Corresponding author.
E-mail addresses: carina.prell@uni-bielefeld.de (C. Prell), sophie-ann.vonderbank@uni-bielefeld.de (S.-A. Vonderbank), florian.meyer@uni-bielefeld.de (F. Meyer), fernando.perez-garcia@ntnu.no (F. Pérez-García), volker.wendisch@uni-bielefeld.de (V.F. Wendisch).

https://doi.org/10.1016/j.crbiot.2021.12.004
Received 29 October 2021; Revised 10 December 2021; Accepted 19 December 2021

Introduction

Microbial enzymes are exceptionally attractive to be incorporated in chemical processes as they are sustainable and environmentally friendly (Sheldon and Woodley, 2018). One major advantage of these biocatalysts is their ability to catalyse interconversions of many functional groups with well-defined selectivity (chemo-, regio-, stereo-) ensuing reduced waste during synthesis and high atom economy. The recent developments in bioinformatics, synthetic biology, and computational biology enabled a deeper understanding of the enzymatic reactions and the establishment of effective biotransformation systems for industrial use (Bornscheuer et al., 2012; Sun et al., 2018). It is important to discover novel enzymes or unknown side activities of known enzymes to access new products, e.g. for the functionalization of non-activated C-H bonds, which are difficult for organic chemists (Bastard et al., 2018). One group of enzymes, which catalyse the formation of various C-heteroatom bonds, are the iron (II)/α-ketoglutarate dependent dioxygenases (KDO) (Hausinger, 2004; Wan et al., 2017), that e.g., hydroxylate C-H bonds (Dunham et al., 2018; Hausinger, 2004). These enzymes require the cofactor iron (II) and three substrates: molecular oxygen, 2-OG and a primary substrate. One oxygen atom is transferred to the primary substrate to yield the hydroxylated product, and the second oxygen is used for oxidation of 2-OG to succinate and carbon dioxide (Bastard et al., 2018; Martinez and Hausinger, 2015; Mitchell et al., 2017). Typical substrates for these metalloenzymes are amino acids, which are hydroxylated. KDOs are mainly involved in the biosynthesis of secondary metabolites and can be found in bacteria, where they hydroxylate the side chains of free amino acid (derivatives) or tether peptides in non-ribosomal peptide biosynthesis (Wu et al., 2016). The hydroxylated amino acids are highly attractive intermediates in pharmaceutical industries and find application as valuable chiral building blocks for fine chemistry (Jing et al., 2021; Ren and Fasan, 2021). KDOs that are active towards amino acids and their derivatives belong to the Clavaminate Synthase Like (CSL) family. They are highly substrate specific and exhibit high regio- and stereoselectivities (Bastard et al., 2018; Hara et al., 2017). Among the KDOs which act specifically on L-lysine, the KDOs from *Catenulispora acidiphila* (Baud et al., 2014; Peters and Buller, 2019) and *Kineococcus radiotolerans* SRS30216 (Hara et al., 2017) yield L-3-hydroxylysine, while the KDOs from *Flavobacterium johnsoniae* UW101 (Bastard et al., 2018; Baud et al., 2014) or *Niastella koreensis* (Wang et al., 2020) show different regioselectivity and form D-4-hydroxylysine.

As the physiological function of hydroxylysine depends on the location of the hydroxyl group, the regio- and stereoselective synthesis is highly important. In nature, the most abundant isomer of hydroxylated lysine is D-5-hydroxylysine and it is found in a particular type of collagen peptide (Peters and Buller, 2019). It frequently occurs in the extracellular matrix of animal cells, where it stabilizes the collagen scaffold by subsequent O-glycosylation. Moreover, L-lysine residues present in proteins can be hydroxylated as a posttranslational modification by lysyl hydroxylase (EC 1.14.11.4) (Turpeenniemi-Hujanen and Myllylä, 1984). 5-hydroxylysine (5-HL) can also be found in bacteria, like *Staphylococcus aureus*, where it is used as a cell-wall precursor instead of lysine (Smith et al., 1965). Moreover, regio- and stereoisomers are highly demanded as synthons for pharmaceutical agents. For example, C3-hydroxylation of L-lysine provides the precursor for synthesis of the building block tambroline (X. Zhang et al., 2018), a precursor of the antibiotic tambromycin (Goering et al., 2016). In addition, L-3-hydroxylysine (3-HL) is an intermediate in the synthesis of (-)-balanol in *Verticillium balanoides*, which is a potent protein kinase C inhibitor (Lampe et al., 1996). L- and D-4-Hydroxylysine (4-HL) are also promising precursors for pharmaceutical agents, like functionalized piperidine-2-ones, which are highly versatile building blocks for the synthesis of many bioactive substances (Herbert et al., 2012). They can also be used for the synthesis of 4-hydroxypipecolic acid, a constituent of certain cyclic peptide antibiotics; palinavir, a potent HIV protease inhibitor (Lamarre et al., 1997), or for the anti-cancer agent Glidobactin A (Amatuni and Renata, 2019).

Like lysine, one of the most industrially relevant amino acids, hydroxylysine could be used as a precursor for chemical synthesis. By decarboxylation of lysine, the C_5-diamine polymer building block cadaverine, also known as 1,5-diaminopentane, can be obtained (Cheng et al., 2018). Using hydroxylysine as substrate would yield hydroxylated cadaverine, which could be incorporated as novel building block for polyamides with new properties. Additional hydroxyl groups are attractive in polymers, as they can undergo various reactions, e.g., esterification. Moreover, they are hydrophilic and can act as initiation sites for ring-opening polymerization of cyclic esters, thus enabling easy access to complex polymers (Gómez and Varela, 2007; Kakwere and Perrier, 2011). Orgueira et al. (2001) showed the production of a hydroxylated polymer derived from the building blocks cadaverine and D-2-hydroxyglutarate (Orgueira et al., 2001). Biomaterials, which are derived from polysaccharides showed promising applications in biomedical realms because of their good biocompatibility on the hydroxyl-enriched material surfaces (Yang and Yang, 2014). For the production of cadaverine several approaches have been established, including efficient whole-cell biocatalysis in *E. coli* (Kim et al., 2019). Furthermore, *C. glutamicum* has been engineered for *in vivo* production of cadaverine by overexpression of the genes coding for different pyridoxal phosphate (PLP) dependent decarboxylases from *E. coli*: CadA (Mimitsuka et al., 2007) and LdcC (Kind et al., 2011). The deletion of *snaA* coding for spermi(di)ne-*N*-

acetyltransferase increased product titers by avoiding *N*-acetylation of cadaverine (Kind et al., 2010; Nguyen et al., 2015b). Further optimisation strategies included the application of synthetic promoter-based expression cassettes and integration of different *ldcC* variants in the genome yielding up to 125 g L^{-1} cadaverine (Kim et al., 2018; Oh et al., 2015). *C. glutamicum* was further engineered to exploit starch, wheat sidestream concentrate hydrolysate (WSCH) and methanol as carbon sources for the production of cadaverine (Burgardt et al., 2021; Leßmeier et al., 2015; Tateno et al., 2009).

In this study, a lysine overproducing *C. glutamicum* strain was chosen to extend the lysine biosynthesis pathway to hydroxylated lysine by overexpression of codon-optimised genes coding for KDOs with different regiospecificity to yield either 3-HL (KDO_{Kr} encoded by Krad_3958 from *K. radiotolerans*) or 4-HL (KDO_{Fj} encoded by Fjoh_3169 from *F. johnsoniae*). To improve production, the effects of cofactor and cosubstrate supply as well as substrate/product export and pH alterations were tested. Since hydroxylated lysines can be decarboxylated *in vitro* to hydroxylated cadaverines by different decarboxylases as demonstrated by Bastard et al. (2018), the substrate specificity of the lysine decarboxylases LdcC (Yamamoto et al., 1997) and CadA (Sabo et al., 1974) from *E. coli* and the predicted 4-hydroxylysine decarboxylase DC_{Fj} (Fjoh_3171) (Bastard et al., 2018) were investigated with regard to produce 3-hydroxycadaverine (3-HC) by decarboxylation of 4-HL (Fig. 1). Additionally, the inverse route was explored with decarboxylation of lysine to cadaverine prior to hydroxylation of cadaverine to yield 3-hydroxycadaverine.

Material and methods

Microorganisms and cultivation conditions

C. glutamicum WT strains were cultivated in lysogeny broth (LB) (Bertani, 1951) supplemented with 25 μg mL^{-1} kanamycin. *C. glutamicum* GRLys1 derived strains were cultivated in brain heart infusion with 0.5 M sorbitol (BHIS), supplemented with 25 μg mL^{-1} kanamycin, 100 μg mL^{-1} spectinomycin or 5 μg mL^{-1} tetracycline, when appropriate. All bacterial strains and plasmids are listed in Tables 1 and 2. Growth experiments with *C. glutamicum* were performed in CGXII minimal medium at pH 7.0 (Eggeling and Bott, 2004) supplemented with 40 g L^{-1} glucose as sole carbon source and induced with 1 mM IPTG if necessary. The amount of iron and the pH were adjusted to 1.04 mM and 6.5, respectively, as indicated in the result section. Overnight cultures were harvested and washed twice in TN buffer (50 mM Tris-HCl, 50 mM NaCl, pH 6.3) before inoculation to an initial OD_{600} of 1. The cultivations in the BioLector microcultivation system (m2p- labs, Baesweiler, Germany) were performed in 3.2 mL FlowerPlates at 30 °C, 1100 rpm and a filling volume of 1000 μL.

Molecular biology methods

Isolation of genomic DNA and classical methods which include plasmid isolation, molecular cloning and heat-shock transformation of *E. coli* and electroporation of *C. glutamicum* were performed as described previously (Eikmanns et al., 1994; Simon et al., 1983).

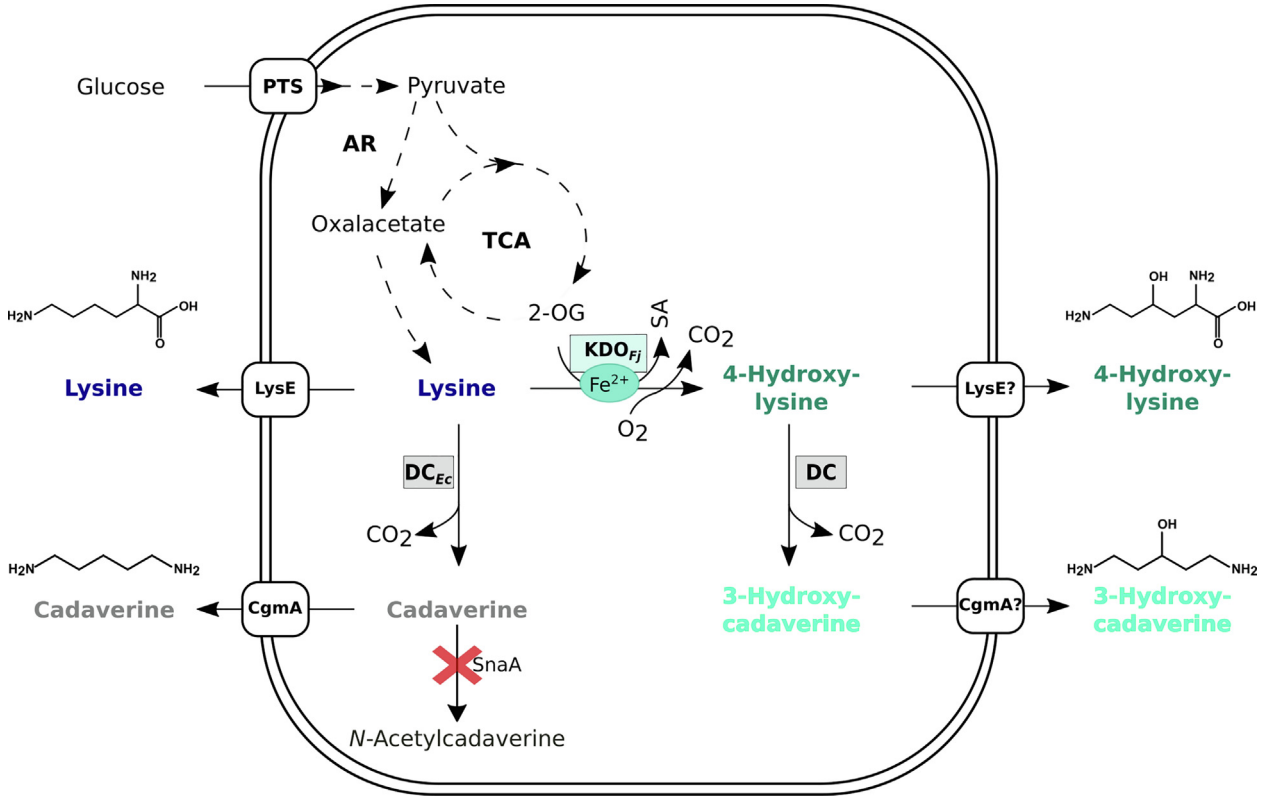

Fig. 1. Schematic overview of the predicted route towards 3-hydroxycadaverine from lysine. Enzymes are depicted next to their reaction. Heterologous proteins are boxed. Deletion of coding gene is marked by a red cross. DC: Decarboxylase from different organisms (lysine decarboxylase from *E. coli* MG1655 (LdcC, CadA), PLP-dependent decarboxylase from *Flavobacterium johnsoniae* UW101 (DC_{Fj})); KDO_{Fj}: α-ketoglutarate dependent dioxygenase/lysine 4-hydroxylase from *Flavobacterium johnsoniae* UW101; SnaA: spermi(di)ne-*N*-acetyltransferase from *C. glutamicum* WT; LysE: lysine/4-HL exporter; CgmA: cadaverine/3-HC exporter, PTS: phosphotransferase system). Question marks display transport systems that may be involved for export of 4-HL and 3-HC, respectively, based on genetic evidence, but in the absence of biochemical evidence. Dashed lines represent multiple reactions. 2-OG: 2-oxoglutarate; SA: succinic acid; TCA: tricarboxylic acid cycle; AR: anaplerotic reaction. (For interpretation of the references to colour in this figure legend, the reader is referred to the web version of this article.)

Table 1
Bacterial strains used in this study.

Strain	Relevant Characteristics	Reference/source
E. coli DH5α	Δ*lac*U169 (φ80*lacZ* ΔM15), *sup*E44, *hsd*R17, *rec*A1, *end*A1, *gyr*A96, *thi*-1, *rel*A1	Hanahan, 1985
C. glutamicum WT	ATCC 13032	ATCC
GRLys1	(DM1933ΔCGP123)	*C. glutamicum* WT with modifications: Δ*pck*, *pyc*^{P458S}, *hom*^{V59A}, 2 copies of *lysC*^{T311I}, 2 copies of *asd*, 2 copies of *dapA*, 2 copies of *dapB*, 2 copies of *ddh*, 2 copies of *lysA*, 2 copies of *lysE*, in-frame deletion of prophages CGP1 (cg1507-cg1524), CGP2 (cg1746-cg1752) and CGP3 (cg1890-cg2071).
		Unthan et al., 2015
GSL	GRLys1 with in-frame deletions: *sugR* (cg2115), *ldhA* (cg3219)	Pérez-García et al., 2018
GSLA	GSL with in-frame deletion: *snaA* (cg1722)	Pérez-García et al., 2018
GSLE2	GSL with deletion of the two copies of *lysE* (cg1424)	Pérez-García et al., 2017
GSLA2	GSLA with in-frame deletion: *cgmA* (cg2893)	Pérez-García et al., 2018
Lys1	GSL (pVWEx4)	This study
Lys2	GSLE2 (pVWEx4) (pEKEx3)	This study
Lys3	GSLE2 (pVWEx4) (pEKEx3-*lysE*)	This study
Lys4	GSL (pVWEx4) (pEKEx3)	This study
Lys5	GSL (pVWEx4) (pEKEx3-*odhI*^{T14A})	This study
Lys6	GSLA (pECXT99A-P$_{syn}$) (pVWEx1)	This study
Lys6Δ*cgmA*	GSLA2 (pECXT99A-P$_{syn}$) (pVWEx1)	This study
HLys1	GSL (pVWEx4-KDO$_{Fj}$)	This study
HLys2	GSLE2 (pVWEx4-KDO$_{Fj}$) (pEKEx3)	This study
HLys3	GSLE2 (pVWEx4-KDO$_{Fj}$) (pEKEx3-*lysE*)	This study
HLys4	GSL (pVWEx4-KDO$_{Fj}$) (pEKEx3)	This study
HLys5	GSL (pVWEx4-KDO$_{Fj}$) (pEKEx3-*odhI*^{T14A})	This study
HLys6	GSLA (pECXT99A-P$_{syn}$-KDO$_{Fj}$) (pVWEx1)	This study
HLys6Δ*cgmA*	GSLA2 (pECXT99A-P$_{syn}$-KDO$_{Fj}$) (pVWEx1)	This study
Cad1	GSLA (pECXT-P$_{syn}$) (pVWEx1-*ldcC*)	This study
Cad2	GSLA (pECXT-P$_{syn}$) (pVWEx1-*cadA*)	This study
Cad3	GSLA (pECXT-P$_{syn}$) (pVWEx1-DC$_{Fj}$)	This study
Cad1Δ*cgmA*	GSLA2 (pECXT-P$_{syn}$) (pVWEx1-*ldcC*)	This study
HCad1	GSLA (pECXT-P$_{syn}$-KDO$_{Fj}$) (pVWEx1-*ldcC*)	This study
HCad2	GSLA (pECXT-P$_{syn}$-KDO$_{Fj}$) (pVWEx1-*cadA*)	This study
HCad3	GSLA (pECXT-P$_{syn}$-KDO$_{Fj}$) (pVWEx1-DC$_{Fj}$)	This study
HCad1Δ*cgmA*	GSLA (pECXT-P$_{syn}$-KDO$_{Fj}$) (pVWEx1-*ldcC*)	This study
GSL (pVWEx4-KDO$_{Kr}$)		This study
WT (pVWEx4)		This study
WT (pVWEx4-KDO$_{Fj}$)		This study
WT (pVWEx1)		This study
WT (pVWEx1-*ldcC*)		This study
WT (pVWEx1-*cadA*)		This study
WT (pVWEx1-DC$_{Fj}$)		This study

ALLin HiFi DNA Polymerase (HighQu, Kraichtal, Germany) was used to amplify DNA sequences with plasmid or genomic DNA as template. The oligonucleotides which were used as primers in this study are listed in Table 3. The genes *cadA* and *ldcC* were amplified from genomic DNA of *E. coli* MG1655 and Fjoh_3171 from *Flavobacterium johnsoniae* UW101 (DSMZ 2064). A standard ribosomal binding site (RBS 5′-GAAAGGAGGCCCTTCAG-3′) was introduced via the respective forward primer. The genes Krad_3958 from *Kineococcus radiotolerans* SRS30216 and Fjoh_3169 from *Flavobacterium johnsoniae* UW101 were codon-optimised (Bio-Rad Laboratories, Hercules, FL, USA) and an optimised RBS was introduced (Salis, 2011). For the variant *odhI*^{T14A} the vector pK19*mobsacB-odhI*^{T14A} was used as a template (Nguyen et al., 2015a). For construction of the overexpression vectors, the respective plasmid was digested with BamHI and assembled with the amplified DNA fragments using Gibson Assembly (Gibson et al., 2009).

Table 2
Plasmids used in this study.

	Relevant Characteristics	Reference
pECXT99A-P$_{syn}$	Tet^R, *C. glutamicum/E. coli* shuttle vector (P$_{syn}$, pGA1 *oriV*$_{Cg}$)	Henke et al., 2021
pECXT99A-P$_{syn}$-KDO$_{Fj}$	pECXT99A-Ps$_{yn}$ expressing KDO$_{Fj}$ from *Flavobacterium johnsoniae* UW101	This study
pEKEx3	Spec^R, *C. glutamicum/E. coli* shuttle vector (P$_{tac}$ *lacI*^{q} pBL1, *oriV*$_{Ec}$)	Stansen et al., 2005
pEKEx3-*odhI*^{T14A}	pEKEx3, expressing *odhI* (cg1630) carrying SNP T14A from *C.glutamicum* WT	This study
pEKEx3-*lysE*	pEKEx3, expressing *lysE* (cg1424) from *C. glutamicum* WT	Lubitz et al., 2016
pVWEx1	Kan^R, *C. glutamicum/E. coli* shuttle vector (P$_{tac}$, *lacI*^{q})	Peters-Wendisch et al., 2001
pVWEx1-*ldcC*	pVWEx1, expressing *ldcC* (CXP41_00970) from *E. coli* MG1655	Jorge et al., 2017
pVWEx1-*cadA*	pVWEx1, expressing *cadA* (CXP41_22535) from *E. coli* MG1655	This study
pVWEx1-DC$_{Fj}$	pVWEx1, expressing Fjoh_3171 from *Flavobacterium johnsoniae* UW101	This study
pVWEx4	Kan^R, *C. glutamicum/E. coli* shuttle vector (P$_{tac}$, *lacI*^{q})	Henke et al., 2021
pVWEx4-KDO$_{Kr}$	pVWEx4 expressing KDO$_{Kr}$ (Krad_3958) from *Kineococcus radiotolerans* SRS30216	This study
pVWEx4-KDO$_{Fj}$	pVWEx4 expressing KDO$_{Fj}$ (Fjoh_3169) from *Flavobacterium johnsoniae* UW101	This study

Quantification of amino acids, carbohydrates and organic acids by HPLC

The quantification of extracellular amino acids, their derivatives and carbohydrates in the cultivation medium was performed with a high-performance liquid chromatography system (1200 series, Agilent Technologies Deutschland GmbH, Böblingen, Germany). After centrifugation of 1 mL of cell cultures at 20238 g for 10 min the supernatant was stored at −20 °C prior to analysis. Analysis of amino acids, diamines and ω-amino acids was performed by an automatic pre-column derivatization with *ortho*-phthaldialdehyde (OPA) and separated on a reversed phase HPLC using a a pre-column (LiChrospher 100 RP18 EC-5μ (40 × 4 mm), CS Chromatographie Service GmbH, Langerwehe, Germany) and a main column (LiChrospher 100 RP18 EC-5μ (125 × 4 mm), CS Chromatographie Service GmbH). A mobile phase of buffer A (0.25% (*v/v*) sodium acetate, pH 6.0) and buffer B (methanol) was used. The following gradient was applied: 0–1 min 20 % B (0.7 mL min^{-1}), 1–11 min a linear gradient of B from 20% to 85% (1.2 mL min^{-1}), 12–13 min a linear gradient of B from 85% to 20% (1.2 mL min^{-1}). To quantify amino acids, diamines and ω-amino acids, the standards of ornithine, lysine, 5-HL, putrescine, cadaverine, GABA and 5AVA were analysed in a range from 50 to 800 μM. The peak area was normalised to the internal standard of 100 μM asparagine (Schneider and Wendisch, 2010) by division of the respective standard peak area by the area of the internal standard.

Table 3
Oligonucleotides used as primers in this study (RBS in **bold**, overlaps in *italic*).

Primer	Sequence (5′ − 3′)	Construct
PC48	*CAGGTCGACTCTAGAGGATTCC***TCGCTCTGCAGCGAACCCGCCTTTTTAAAAGGAGGTTTTTTT**ATGTCCTCCCTGTTCC	pVWEx4- KDO_{Kr}
PC49	*GAATTCGAGCTCGGTACCCGGGGATC*TTAGGAGAAGGATGCCTG	
PC52	*CAGGTCGACTCTAGAGGATTCC***TATAAATAGCCCCATCGCTCTTGGGGTAAAAAGGAGGTATTTT**ATGAAGTCCCAGTCC	pVWEx4- KDO_{Fj}
PC53	*GAATTCGAGCTCGGTACCCGGGGATC*TTATGCCTGGTCGAAAAC	
CA24	*GCCTGCAGGTCGACTCTAGAG***GAAAGGAGGCCCTTCAG**ATGAGCGACAACAACGGC	pEKEx3-$odhI^{T14A}$
CA25	*AATTCGAGCTCGGTACCCGGGGATC*TTACTCAGCAGGGCCTGC	
CA26	*GAATTCGAGCTCGGTACCCGGG***TATAAATAGCCCCATCGCTC**	pECXT99A-P_{syn}- KDO_{Fj}
CA27	*CCTGCAGGTCGACTCTAGAGGATC*TTATGCCTGGTCGAAAAC	
CA28	*CCTGCAGGTCGACTCTAGAGGATTCC***GAAAGGAGGCCCTTCAG**ATGCAAAACCTATTAGACAATGCC	pVWEx1-DC_{Fj}
CA29	*ATTCGAGCTCGGTACCCGGGGATTCC*TTAGGAGAAGATGTAGTCATTTCCG	
CA31	*CCTGCAGGTCGACTCTAGAGGATTCC***GAAAGGAGGCCCTTCAG**ATGAACGTTATTGCAATATTGAATC	pVWEx1-*cadA*
CA32	*ATTCGAGCTCGGTACCCGGGGATTCC*TTATTTTTTGCTTTCTTCTTTCAA	

The area quotient was plotted against the concentration of the respective standard. The slope of the calibration curve was used to quantify the respective substance. As C3/C4-hydroxylated lysine and C2/C3-hydroxylated cadaverine are not commercially available, 3-HL/4-HL/4,5-DHL and 2-HC/3-HC were quantified as equivalents. To determine 3-HL, 4-HL and 4,5-DHL concentrations, the slope of 5-HL standard calibration curve was used, and concentrations were given as 5-HL equivalents. To determine 2-HC and 3-HC, the slope of cadaverine standard calibration curve was used, and concentrations were given as cadaverine equivalents. Detection of the fluorescent derivatives was carried out with a fluorescence detector (FLD G1321A, 1200 series, Agilent Technologies, Waldbronn, Germany) with an excitation wavelength of 230 nm and an emission wavelength of 450 nm. Glucose and 2-oxoglutarate concentrations were measured with an anion exchange column (Aminex, 300 mm × 8 mm, 10 µm particle size, 25 Å pore diameter, CS Chromatographie Service GmbH, Langerwehe, Germany) under isocratic conditions (5 mM H_2SO_4) at 60 °C with a flow of 0.8 mL min^{-1} as described previously (Schneider et al., 2011). The substances were detected with a refractive index detector (RID G1362A, 1200 series, Agilent Technologies, Waldbronn, Germany).

Determination of substrate specificity via biotransformation

Pellets from *C. glutamicum* strains WT (pVWEx1), WT (pVWEx1-*ldcC*), WT (pVWEx1-*cadA*), WT (pVWEx1-DC_{Fj}), WT (pVWEx4) and WT (pVWEx4-KDO_{Fj}) were obtained from cultivations in 50 mL CGXII minimal medium supplemented with 20 g L^{-1} glucose, 1 mM IPTG and 25 µg mL^{-1} kanamycin. The pellets were washed twice in 20 mL 50 mM HEPES buffer (pH 7.5) and centrifuged for 10 min at 4000 rpm and 4 °C and resuspended in 2 mL of 50 mM HEPES buffer (pH 7.5). Cells were disrupted by sonication (cycle. 0.5, amplitude of 55%) on ice for 9 min. To remove cells debris, centrifugation was performed for 1 h at 20238 g and 4 °C. The crude extract was used for the biocatalytic reaction. Protein concentrations were determined with the Bradford assay kit (Bio-Rad Laboratories, Hercules, CA, United States) using BSA (bovine serum albumin) as standard.

The determination of the biocatalytic activity of the hydroxylase was performed as described before (Baud et al., 2017, 2014). 1.5 mL reaction mix contained 50 mM HEPES buffer (pH 7.5), 15 mM 2-oxoglutarate, 2.5 mM ascorbate, 1 mM ammonium iron (II) sulfate and 10 mM of the respective substrate (lysine, 5-HL, ornithine, putrescine, cadaverine, GABA, 5AVA). The reaction was started by addition of 2 mg mL^{-1} protein. The reaction mixture was stirred at 30 °C in Duetz microcultivation plates (Kuhner Shaker GmbH, Herzogenrath, Germany) with culture volumes of 1.5 mL at 300 rpm in an Ecotron ET25-TA-RC (Infors HT, Einsbach, Germany) and plate sandwich covers for low evaporation (1.2 mm hole diameter) were used. Samples were taken after 24 h. Proteins from the crude extract were precipitated with trichloroacetic acid (TCA). 50 µL 100% (*w/v*) TCA were added to 500 µL of sample and incubated for 30 min on ice (Koontz, 2014). After centrifugation at 20238 g for 10 min, the supernatant was neutralized with NaOH and stored at − 20 °C prior to analysis. The product formation was determined by HPLC.

To identify the substrate specificity of the different decarboxylases the following assay was performed: 1.5 mL reaction mix contained 50 mM HEPES buffer (pH 7.5), 1 mM PLP, 1 mM DTT and 10 mM of the respective substrate (lysine, 5-HL, 4-HL from fermentation broth) (Baud et al., 2017). The reaction was started by addition of 1 mg mL^{-1} protein. Incubation of the reaction mix, sampling, sample treatment and analysis were performed as described for the KDO assay.

Fermentative production of 3-HC

A baffled bioreactor with a total volume of 3.6 L was used for scale-up experiments (KLF, Bioengineering AG, Switzerland). Two six-bladed Rushton turbines were placed on the stirrer axis with a distance from the bottom of the reactor of 6 and 12 cm. The stirrer to reactor diameter ratio was 0.39. The dissolved oxygen concentration in the batch phase was kept at a minimum of 30% by stepwise increases of the stirrer rate. A constant airflow of 0.75 L min^{-1} was maintained from the bottom through a sparger, corresponding to an aeration rate of 0.75 vvm. The pH was kept constant at 6.50 ± 0.05 by automatic addition of phosphoric acid (10% (*v/v*)) and ammonia (25 % (*w/v*)). The temperature was maintained at 30 °C. To prevent foaming 0.6 mL L^{-1} of the antifoam agent AF204 (Sigma Aldrich, Darmstadt, Germany) was added, and a mechanical foam breaker was present to serve as an additional foam control. The fermentation was performed with a head space overpressure of 0.5 bar. The initial working volume of 1 L was inoculated to an OD_{600} of 1.5 from a shake flask pre-culture in CGXII minimal medium (pH 6.5) supplemented with 40 g L^{-1} glucose and 1.5 mM $FeSO_4$. Samples were collected by an autosampler and cooled down to 4 °C until further use. The feed consisted of 400 g L^{-1} glucose, 0.75 g L^{-1} $MgSO_4 \cdot 7H_2O$ and 1.5 mM $FeSO_4$ (ρ = 1.15 kg m^{-3}). The feed was applied at 1.2 mL min^{-1} as long as the pO_2 surpassed 60%. If the feed-pump was constantly active for more than 1 min, the feed was halted to prevent overfeeding. The plasmid-based overexpression of *ldcC* was induced with 1 mM IPTG after 24 h.

Results

Determination of the substrate spectra of the lysine-4-hydroxylase KDO_{Fj}

Hydroxylases are known for their high substrate specificity. Therefore, it is essential to test if non-natural substrates like cadaverine can be accepted. It was shown before that the lysine-4-hydroxylase KDO_{Fj} can accept 5-HL and convert it to 4,5-dihydroxylysine (4,5-DHL) with a low efficiency of 15 % conversion next to its natural substrate lysine (65 % conversion) (Baud et al., 2014), but not ornithine. In this study, the diamines cadaverine and putrescine as well as the ω-amino acids γ-

aminobutyrate (GABA) and 5-aminovalerate (5AVA) were tested as well. Indeed, it could be confirmed that 79% of the added lysine was converted to 4-hydroxylysine using crude extract of *C. glutamicum* WT (pVWEx4-KDO$_{Fj}$) within 24 h (Table 4). Moreover, 4,5-DHL could be produced from 5-HL. However, none of the other substrates was hydroxylated (Table 4, Figure S1, Table S1). Thus, as cadaverine was not hydroxylated by KDO$_{Fj}$, conversion of lysine to 3-HC had to occur in a reaction sequence with lysine hydroxylation occuring before 4-HL decarboxylation.

Determination of the substrate specificity of different lysine decarboxylases

The capability of different PLP-dependent decarboxylases to decarboxylate lysine and hydroxylated lysines was tested. It was described before that the decarboxylase from *Flavobacterium johnsoniae* DC$_{Fj}$ decarboxylates 4-HL with high efficiency, but not 5-HL (Baud et al., 2017). Crude extract of *C. glutamicum* WT (pVWEx1-DC$_{Fj}$) converted 4-HL (18 % of 10 mM), whereas neither 5-HL nor lysine were decarboxylated within 24 h (Table 5, Figure S2, Table S1). By contrast, CadA and LdcC from *E. coli* fully converted lysine and 4-HL within 24 h (Table 5) yielding cadaverine and 3-HC, respectively. Only about 50% of 10 mM 5-HL was converted to 2-hydroxycadaverine by LdcC and CadA (Table 5).

Fermentative production of hydroxylated lysines via regiospecific C-H-hydroxylation using different KDOs

Lysine biosynthesis in *C. glutamicum* was extended by regiospecific hydroxylases (KDOs) to produce hydroxylated lysines fermentatively. C. *glutamicum* strain GSL was chosen as base strain, as this lysine overproducer has been successfully engineered to produce lysine-derived compounds (Pérez-García et al., 2018, 2017; Prell et al., 2021). By addition to growth medium, 5-HL was shown neither to be toxic to *C. glutamicum* GSL nor to be catabolized (data not shown). Genes encoding two KDOs showing different regioselectivity were tested. To obtain 3-HL a codon-optimised version of Krad_3958 (KDO$_{Kr}$) from *K. radiotolerans* was heterologously overexpressed in GSL, whereas for 4-HL production a codon-optimised version of Fjoh_3169 (KDO$_{Fj}$) was used. In shake flask cultivation, 3 ± 1 mM 3-HL was accumulated by GSL (pVWEx4-KDO$_{Kr}$) with concomoitant production of 35 ± 3 mM lysine (Fig. 2B). In contrast, overexpression of KDO$_{Fj}$ led to a higher 4-HL concentration (23 ± 1 mM) and a lower lysine (15 ± 2 mM) concentration (Fig. 2B). Biomass formation of both producers was comparable to the empty vector carrying strain GSL (pVWEx4), whereas the growth rate was significantly reduced in the 4-HL producer (μ= 0.20 ± 0.00 h^{-1}) compared to the control strain (μ= 0.25 ± 0.02 h^{-1})- and the 3-HL producer (Fig. 2A). Since 4-HL production led to higher titers than 3-HL production, production of 4-HL was further optimised and the strains GSL (pVWEx4) and GSL (pVWEx4-KDO$_{Fj}$) were named Lys1 and HLys1, respectively.

Table 4
Substrate specificity of lysine-4-hydroxylase KDO$_{Fj}$ in 2 mg mL^{-1} crude extract after 24 h (n.c. = not converted).

Enzyme	Substrate [10 mM]	Conversion [%]
Lysine-4-hydroxylase	Lysine	79
	5-Hydroxylysine	14
	Ornithine	n.c.
	Putrescine	n.c.
	Cadaverine	n.c.
	γ-Aminobutyrate	n.c.
	5-Aminovalerate	n.c.

Table 5
Conversion of selected compounds by decarboxylases from different organisms by 1 mg mL^{-1} crude extract after 24 h (n.c. = not converted).

Enzyme	Substrate [10 mM]	Conversion [%]
LdcC	Lysine	98
	5-Hydroxylysine	48
	4-Hydroxylysine	100
CadA	Lysine	98
	5-Hydroxylysine	50
	4-Hydroxylysine	100
DC$_{Fj}$	Lysine	n.c.
	5-Hydroxylysine	n.c.
	4-Hydroxylysine	18

Role of LysE for 4-hydroxylysine production

Transport engineering is a promising approach for optimising producer strains (Krämer, 2002; Pérez-García and Wendisch, 2018). For example, overexpression of the gene coding for the lysine exporter LysE accelerated lysine production (Gunji and Yasueda, 2006), while its deletion improved production of the lysine-derived L-pipecolic acid by minimizing loss of lysine as precursor of L-pipecolic acid (Pérez-García et al., 2017). Strains unable to export lysine while oversynthesizing it suffer from growth perturbation (Pérez-García et al., 2017) as up to 1 M lysine may accumulate intracellularly as consequence of such metabolic imbalance (Vrljic et al., 1996). Growth perturbation may be overcome by conversion of lysine to another compound that is exported independently of LysE, e.g. conversion of lysine to L-pipecolic acid (Pérez-García et al., 2017). To test if the deletion of *lysE* might affect 4-HL production, strain GSLE2 which lacks *lysE* was used. As expected, the absence of LysE severely perturbed growth of the lysine producer GSLE2 (pVWEx4) (pEKEx3) (=Lys2) (Table 6). Growth of the 4-HL producer GSLE2 (pVWEx4-KDO$_{Fj}$) (pEKEx3) (=HLys2) was severely perturbed under the tested conditions as well (Table 6). When both strains were complemented by plasmid-based overexpression of *lysE*, (strains named Lys3 and HLys3) growth, accumulation of lysine (16 ± 1 mM) as well as of 4-HL (2 ± 0 mM) in the supernatant were restored (Table 6). Thus, unlike conversion of lysine to L-pipecolic acid in the absence of LysE (Pérez-García et al., 2017), conversion of lysine to 4-HL did not restore growth in the absence of LysE (Table 6). One may speculate that LysE is not only exporting lysine, arginine and citrulline out of the *C. glutamicum* cell (Lubitz et al., 2016), but may also be involved in export of 4-HL.

Effect of increased supply of 2-oxoglutarate as cosubstrate on 4-HL production

It was demonstrated before that sufficient supply of the cosubstrate 2-OG is crucial to facilitate hydroxylation of amino acids catalysed by KDOs. By dynamic modulation of the 2-oxoglutate dehydrogenase complex (ODHC) in *C. glutamicum* production of 4-hydroxyisoleucine (C. Zhang et al., 2018) and *trans*-4-hydroxyproline (Long et al., 2020) were improved. In this study, the impact of extracellularly added 2-OG on 4-HL production in HLys1 was investigated first. Increased biomass formation and a decreased growth rate were only observed at 60 mM 2-OG (Fig. 3A). Notably, 2-OG concentrations remained stable when 30 mM or less 2-OG were added, but 2-OG appeared to be catabolised at 45 mM and 60 mM (Fig. 3A). The addition of 30 mM 2-OG or more only resulted in a minor increase from 20 ± 0 mM up to 22 ± 0 mM 4-HL. Interestingly, the lysine concentrations gradually decreased from 14 ± 0 mM to 7 ± 1 mM with increasing 2-OG concentrations up to 60 mM. Therefore, addition of 2-OG hardly affected 4-HL titers but was beneficial as it decreased production of lysine as major by-product (Fig. 3B).

As a next step, supply of 2-OG was adjusted by overexpression of the gene *odhI*^{T14A} coding for the inhibitor of the ODHC with a T14A

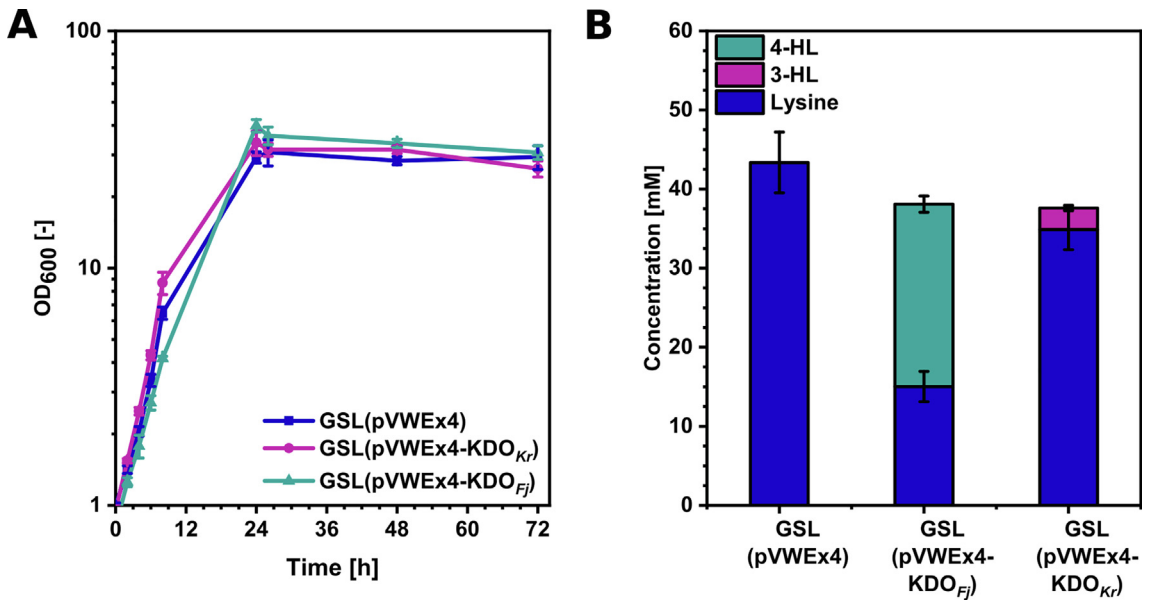

Fig. 2. Production of hydroxylated lysines by overexpression of different KDOs. Comparison of (**A**) growth and (**B**) production of the lysine producer GSL (pVWEx4) (blue squares) with 3-HL producer GSL (pVWEx4-KDO$_{Kr}$) (violet circles) and 4-HL producer GSL (pVWEx4-KDO$_{Fj}$) (turquoise triangles). The strains were grown in CGXII minimal medium with 40 g L^{-1} glucose supplemented with 1 mM IPTG in 500 mL baffled shake flasks. The supernatants were analysed after 72 h. Values and error bars represent means and standard deviations (n = 3 cultivations). (For interpretation of the references to colour in this figure legend, the reader is referred to the web version of this article.)

Table 6
Production and biomass formation by *lysE* deficient strains Lys2 and HLys2 in comparison to the complemented strains Lys3 and HLys3 (n.d. = not detectable).

Strain	ΔOD$_{600}$ [-]	Lysine [mM]	4-HL [mM]
Lys2	not grown	n.d.	n.d.
Lys3	23 ± 1	16 ± 1	n.d.
HLys2	not grown	n.d.	n.d.
HLys3	28 ± 2	14 ± 0	2 ± 0

amino acid exchange (Nguyen et al., 2015a). The amino acid exchange abolishes phosphorylation of one of two phosphorylation sites, thus, increasing inhibition of ODHC which requires unphosphorylated OdhI. Indeed, the overexpression of *odhI*^{T14A} resulted in a 4.4-fold increase of 2-OG accumulation in the culture broth (31 ± 1 mM) by *C. glutamicum* Lys5 in comparison to the control strain Lys4 with 7 ± 0 mM (Fig. 3D). Concomitantly, the glutamate titers were increased (23 ± 1 mM compared to 10 ± 0 mM), while lysine production (60 ± 1 mM compared to 37 ± 2 mM) (Fig. 3D) and the growth rate (0.18 ± 00 h^{-1} compared to 0.14 ± 00 h^{-1} decreased (Fig. 3C). Overexpressing *odhI*^{T14A} also affected growth by the 4-HL producer HLys5 (Fig. 3C). While the glutamate concentrations accumulated by both strains were similar (7 ± 0 mM by HLys4 and 6 ± 1 mM by HLys5), about 2-fold more 2-OG accumulated in *odhI*^{T14A} overexpressing 4-HL producing strain HLys5 (Fig. 3D). However, about 2- to 3-fold less 4-HL were produced, but more about 2-fold more lysine accumulated. Thus, modulating ODHC activity by overexpressing *odhI*^{T14A} did not improve 4-HL production.

Effect of increased supply of iron as cofactor on 4-HL production

The influence of the KDO cofactor iron (II) was investigated since it was shown before that elevated concentrations of iron (II) in the cultivation medium improved production of L-2-hydroxyglutarate by *C. glutamicum* significantly which involved hydroxylation of glutarate (Prell et al., 2021). Therefore, up to 2.5 mM iron sulfate were added to the CGXII minimal medium, which already contained 37 μM Fe^{2+}. Addition of iron sulfate to the growth medium slowed growth of strains Lys1 and HLys1 (Fig. 4A; K_i = 1.9 mM for Lys1 and K_i = 1.3 mM for HLys1). Lysine production by Lys1 was increased by addition of 0.5 mM or more iron sulfate (Fig. 4B). Of note, gradually increasing the addition of iron sulfate to the culture broth of HLys1 reduced lysine accumulation and increased 4-HL production proportionally (Fig. 4D). When 1.0 mM Fe^{2+} were added, HLys1 produced 29 ± 1 mM 4-HL, but only 6 ± 0 mM lysine in comparison to standard cultivation conditions (20 ± 0 mM 4-HL, 14 ± 0 mM lysine) (Fig. 4D). Since at 2.5 mM Fe^{2+} only slightly more 4-HL titer (32 ± 1 mM) were produced, but the growth rate dropped to 0.07 ± 0.00 h^{-1}, addition of 1.0 mM Fe^{2+} was chosen for the following experiments since the growth rate was still 0.11 ± 0.00 h^{-1}.

Adaption of extracellular pH for improved precursor supply and 4-HL production

For KDO$_{Fj}$ various pH values ranging from 6.0 (Hara et al., 2017) to 7.5 (Baud et al., 2014) were described as optimal condition for the enzymatic reaction of the purified protein. Although pH homeostasis of *C. glutamicum* is effective in this pH range (Jakob et al., 2007), the influence of the external pH on lysine and 4-HL production was investigated. Growth of HLys1 was affected stronger at pH 6.5 than that of Lys1 (Fig. 5A, C). Lysine production by Lys1 was decreased from pH 6.5 (65 ± 5 mM) to pH 7.5 (47 ± 3 mM), while lysine production by HLys1 was affected less by the medium pH (Fig. 5B, D). Notably, 4-HL production was maximal at pH 6.5 with a titer of 54 ± 4 mM and only 9 ± 1 mM lysine accumulating as a by-product (Fig. 5D). Although slow growth was observed at pH 6.5, this medium pH supported the highest 4-HL titers with the least accumulation of lysine as by-product. Thus, pH 6.5 was chosen as standard for the following experiments.

Extension of the pathway from 4-HL to 3-HC

Cadaverine and potentially 3-HC are *N*-acetylated by spermi(di)ne-*N*-acetyltransferase (Nguyen et al., 2015b). Therefore, the respective

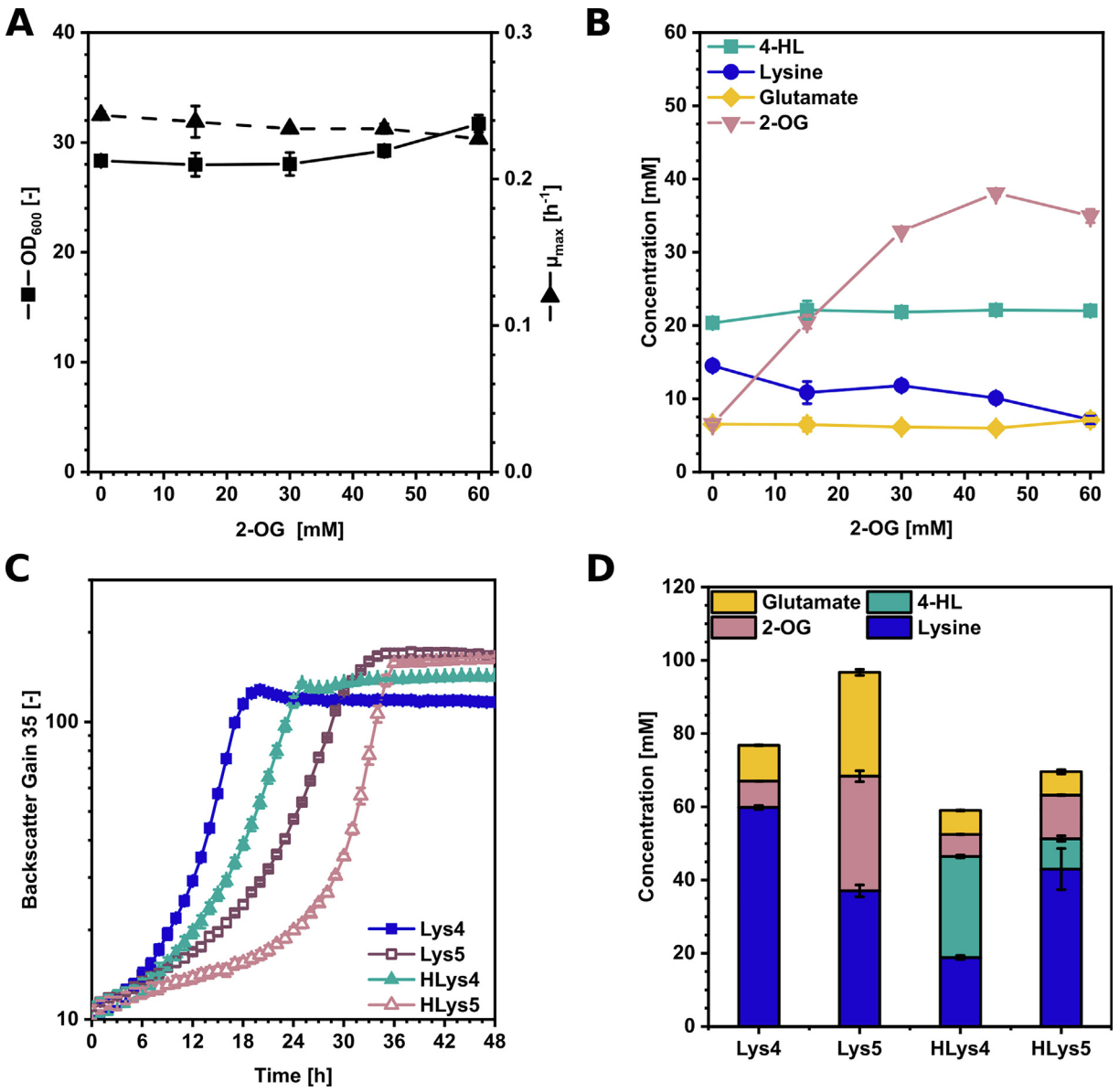

Fig. 3. Effect of 2-oxoglutarate on 4-HL production. Effect of extracellularly added 2-OG on (**A**) OD_{600} (black squares), and maximum growth rates (black traingles) and (**B**) production of lysine (blue circles), 4-HL (turquoise squares), glutamate (yellow diamonds) and 2-OG (brown triangles) by HLys1. (**C**) Growth and (**D**) production of the lysine producer Lys4 (blue squares) and the 4-HL producer HLys4 (turquoise triangles) in comparison to the strains Lys5 (dark brown empty squares) and HLys5 (brown empty triangles) overexpressing *odhI*^{T14A}.The strains were cultivated in the Biolector microcultivation system in CGXII minimal medium supplemented with 40 g L^{-1} glucose and 1 mM IPTG. For the cultivation of HLys1 (A, B) increasing 2-oxoglutarate concentrations (0, 15, 30, 45, 60 mM) were added. Supernatants were analysed after 48 h. Values and error bars represent means and standard deviations (n = 3 cultivations). (For interpretation of the references to colour in this figure legend, the reader is referred to the web version of this article.)

gene *snaA* was deleted and the strain carrying the empty vectors pECXT-P_{syn} and pVWEx1 was called Lys6. Strain HLys6 expressed the KDO_{Fj} gene under a strong synthetic promoter (P_{syn}) on plasmid pECXT-P_{syn}. The genes coding for the different decarboxylases LdcC, CadA and DC_{Fj} were expressed under the control of an IPTG-inducible promoter on plasmid pVWEx1 either in Lys6 (yielding strains Cad1-3) or in HLys6 yielding strains HCad1-3). Lys6 produced 89 ± 4 mM lysine, whereas overexpression of the KDO_{Fj} in HLys6 resulted in 36 ± 0 mM 4-HL and 40 ± 9 mM lysine as by-product (Fig. 6A). Plasmid-based overexpression of *ldcC* (Cad1) resulted in 100 ± 5 mM cadaverine with only 1 ± 0 mM lysine as by-product (Fig. 6). Upon overexpression of *cadA* (Cad2) 39 ± 2 mM cadaverine and 53 ± 4 mM lysine accumulated. As expected, no cadaverine, but 73 ± 1 mM lysine was produced by Cad3 as DC_{Fj} cannot accept lysine as substrate.

Strains HCad1-3 that expressed the lysine-4-hydroxylase gene in combination with one of the genes coding for the different decarboxylases (HCad1: *ldcC*; HCad2: *cadA*; HCad3: DC_{Fj}) produced 3-HC to varying degrees (Fig. 6A). HCad2 produced 1 ± 0 mM 3-HC, 30 ± 3 mM cadaverine, 15 ± 1 mM 4-HL and 36 ± 2 mM lysine (Fig. 6A). As expected, HCad3 produced no cadaverine since decarboxylase DC_{Fj} is highly specific for 4-HL, but 2 ± 0 mM 3-HC, 16 ± 0 mM 4-HL and 56 ± 3 mM lysine accumulated. The highest titer of 11 ± 0 mM 3-HC was obtained with HCad1 (Fig. 6). While lysine and 4-HL were no significant by-products, but 72 ± 2 mM cadaverine accumulated. Taken together, 3-HC production by strain HCad1 was investigated further.

Hydroxylation of lysine to 4-HL and subsequent decarboxylation of 3-HC competes with lysine decarboxylation and export of cadaverine as by-product. Thus, *cgmA* coding for the cadaverine exporter was

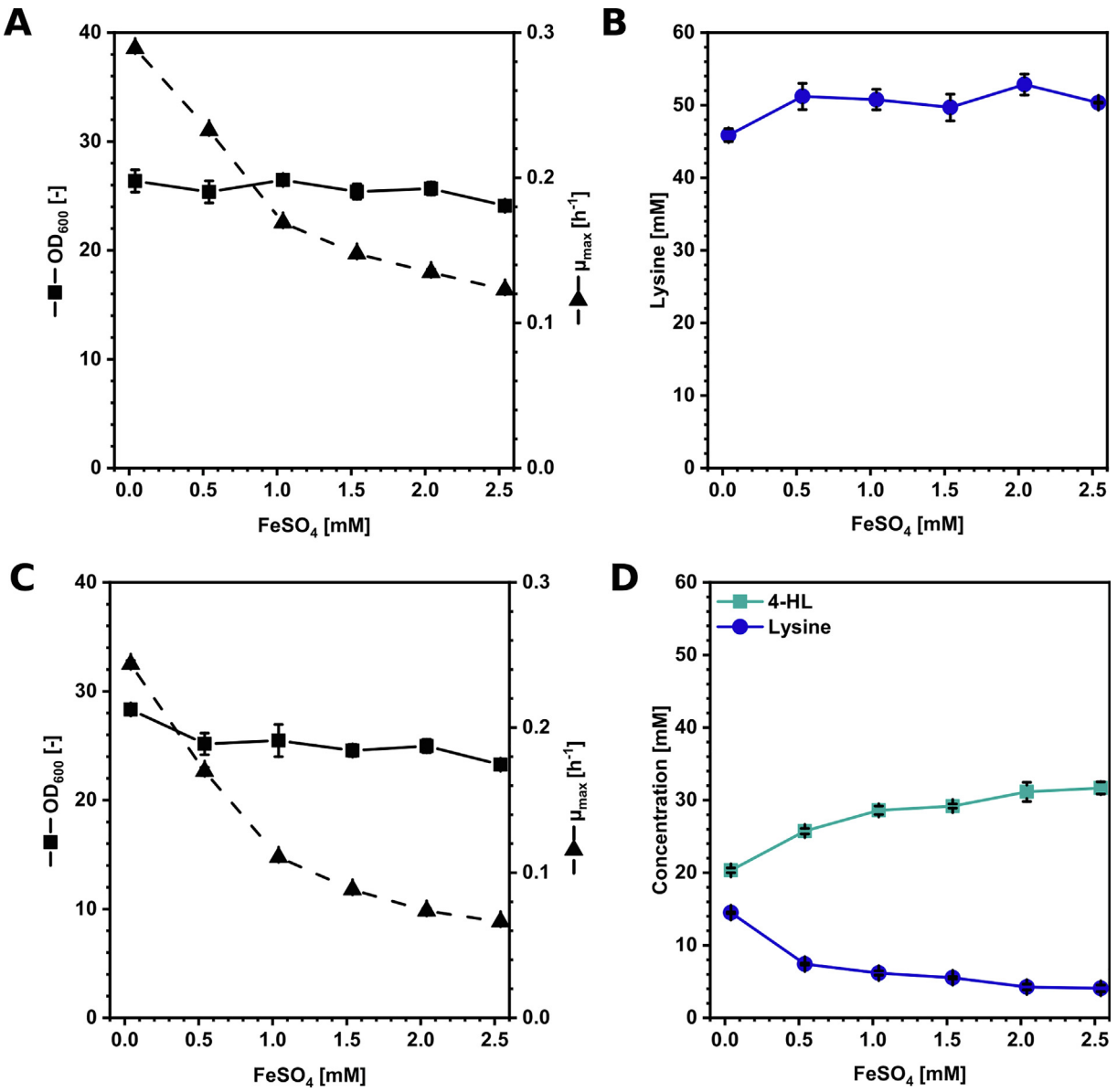

Fig. 4. Effect of iron (II) on (A,C) OD_{600} (black squares), maximum growth rate (black triangles) and (B,D) lysine (blue circles)/4-HL (turquoise squares) production in Lys1 and HLys1. The strains were cultivated in the Biolector microcultivation system in CGXII minimal medium supplemented with 40 g L^{-1} glucose, 1 mM IPTG and increasing iron (II) concentrations (0.04, 0.54, 1.04, 1.54, 2.04, 2.54 mM). Supernatants were analysed after 48 h. Values and error bars represent means and standard deviations (n = 3 cultivations). (For interpretation of the references to colour in this figure legend, the reader is referred to the web version of this article.)

deleted. As consequence, export of cadaverine was almost completely abolished. Moreover, 3-HC was no longer exported in HCad1Δ*cgmA* and only lysine (46 ± 2 mM) and 4-HL (17 ± 2 mM) were detected in the supernatant (Fig. 6B). These results indicated that CgmA might also be the exporter for 3-HC. Thus, deletion of *cgmA* could not be used to avoid accumulation of cadaverine during 3-HC production.

Fermentative production of 3-HC in reactor scale

A 1 L bioreactor cultivation was performed to test if 3-HC production is stable and if operation in the fed-batch mode provides a means to reduce cadaverine formation as by-product. During the batch phase, the aeration rate was kept at 0.75 vvm since this supported 4-HL production using KDO_{Fj} best (data not shown). After 21.5 h the feed started and 1 mM IPTG was added to induce the expression of *ldcC* after 24 h. The cells grew in the batch phase with a growth rate of 0.13 h^{-1} to an OD_{600} of 29 (Fig. 7). In the feed phase, a maximum OD_{600} of 114 was reached after 42 h. After that, the rDOS steadily rose up to 85%, and no more feed was applied. After 44.5 h nitrogen was added manually using the base pump. The decrease in the rDOS led to the addition of more feed solution indicating that nitrogen might be the limiting factor. Even though more feed was applied, no cell growth and further product accumulation could be observed. After 42 h, 74 mM 3-HC (8.8 g L^{-1}, corresponding to 11.4 g L^{-1} when normalized to the initial volume of 1 L) was produced with a volumetric productivity of 1.55 g L^{-1} h^{-1} (corresponding to 2.0 g $L^{-1}h^{-1}$ when normalized to the initial volume of 1 L) and a product yield on biomass of 0.31 g per g CDW (Fig. 7). The product yield on substrate was low (0.07 g g^{-1}) as cadaverine accumulated as main by-product (390 mM; 39.8 g L^{-1}) besides 4-HL (25 mM; 4.1 g L^{-1}). Taken together, compared to the microscale cultivation (11 mM; 1.3 g L^{-1}, 0.44 g L^{-1} h^{-1}, 0.03 g g^{-1}, Fig. 6), the bioreactor fed-batch cultivation enabled a 7-

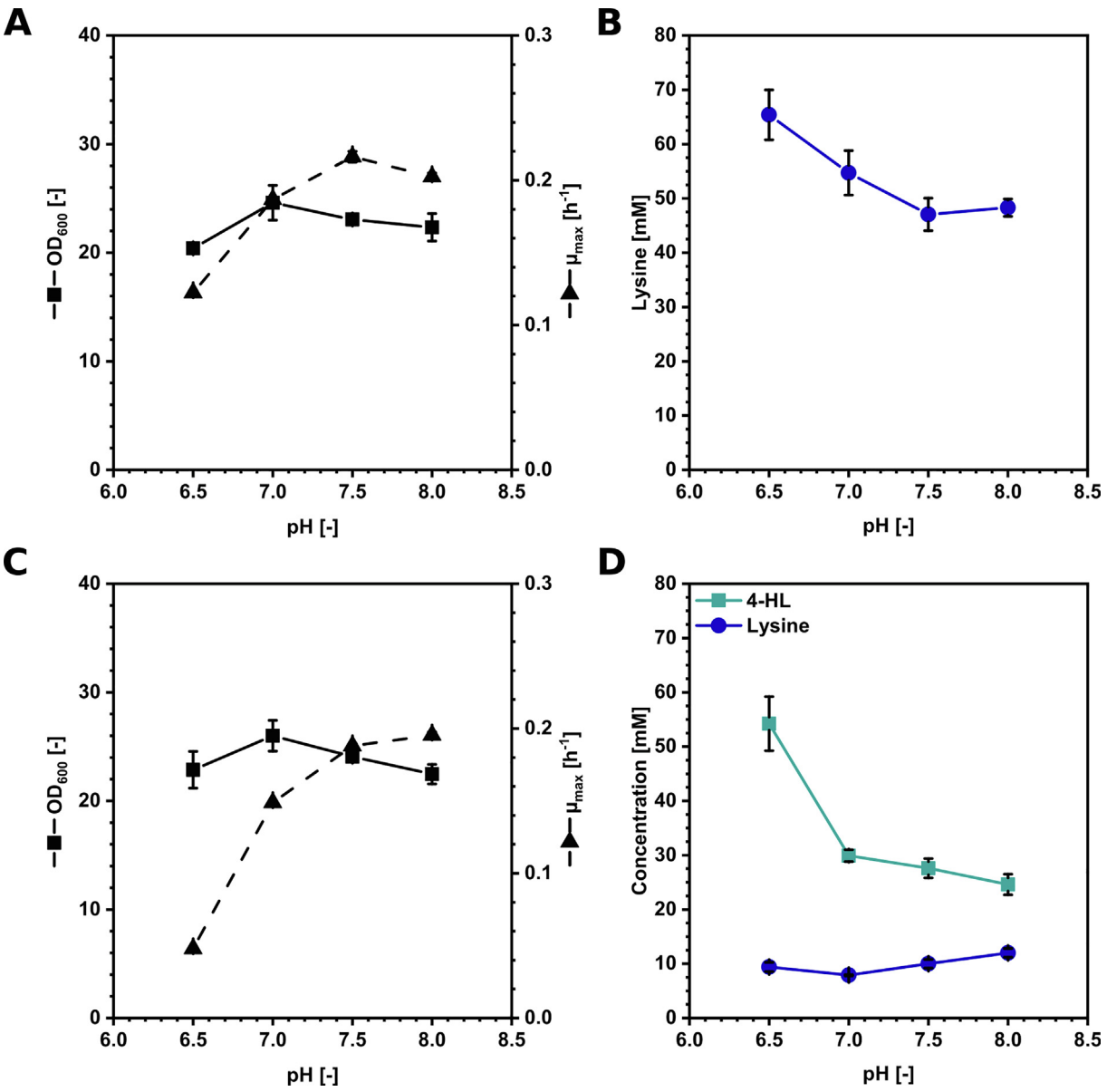

Fig. 5. Effect of pH on lysine and 4-HL production. Comparison of OD_{600} (black squares), maximum growth rate (black triangles) and production of lysine (blue circles) and 4-HL (turquoise squares) in Lys1 (**A, B**) and HLys1 (**C, D**). The strains Lys1 and HLys1 were cultivated in the Biolector microcultivation system in CGXII minimal medium at different pH (6.5, 7.0, 7.5, 8.0) supplemented with 40 g L^{-1} glucose, 1.04 mM $FeSO_4$ and 1 mM IPTG. Supernatants were analysed after 48 h. Values and error bars represent means and standard deviations (n = 3 cultivations). (For interpretation of the references to colour in this figure legend, the reader is referred to the web version of this article.)

fold higher 3-HC titer, a 3.5-fold higher volumetric productivity, and more than 2-fold higher product yield on substrate.

Discussion

In this study, *C. glutamicum* was engineered to produce 4-HL and 3-HC by fermentation. Lysine biosynthesis was extended first by lysine-4-hydroxylase to yield 4-HL and second by a decarboxylase (*E. coli* LdcC > *E. coli* CadA > DC_{Fj} from *F. johnsoniae*) for 3-HC production. To reduce formation of cadaverine as by-product, two-phasic fed-batch cultivation in which KDO_{Fj} was expressed constitutively, whereas expression of *ldcC* was induced when the feed was started, resulted in production of 8.8 g L^{-1} 3-HC (Fig. 7).

The observation that decarboxylation of cadaverine and 4-HL are comparable *in vitro* (Table 5), while more cadaverine, but much less 3-HC accumulated *in vivo* (Fig. 6) points to the conclusion that lysine hydroxylation is the bottleneck of 3-HC production. This may be explained by cadaverine being derived from lysine by direct decarboxylation, whereas 3-HC formation depends on two consecutive reactions: lysine hydroxylase followed by decarboxylase. Thus, there is a need to identify more efficient lysine-4-hydroxylases. The lysine-4-hydroxylase KDO_{Fj} accepts lysine and with lower affinities 3-HL and 5-HL with low efficiency as substrates *in vitro*, but not ornithine (Baud et al., 2014; Hara et al., 2017). Hydroxylation of simple (di)amines such as cadaverine is not possible, likely because a conserved arginine residue interacts with the carboxylate group of lysine via a salt bridge (Baud et al., 2014). The α-amino group of lysine is directly involved in the lid closure via an H-bond with Asn232, which may be relevant for substrate binding (Strieker et al., 2007), i.e. the lid is in its opened-form in the absence of substrates, while it is in closed form when lysine is bound (Bastard et al., 2018). Our finding that

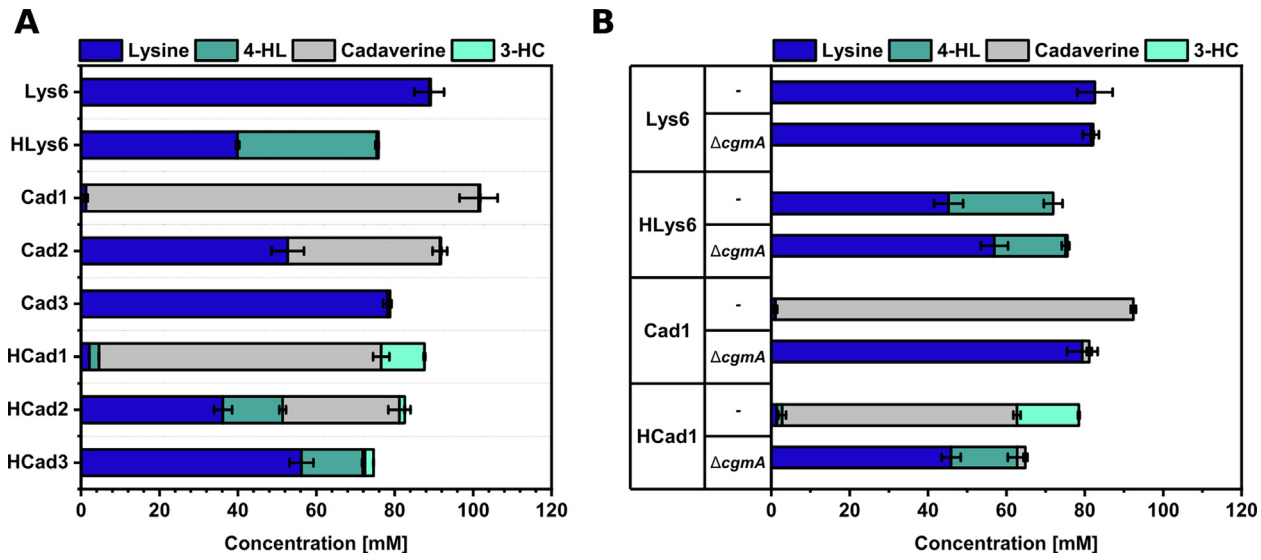

Fig. 6. Comparison of different decarboxylases for production of 3-hydroxycadaverine (A) and impact of deleting the gene coding for the export system CgmA (B). The strains were cultivated in the Biolector microcultivation system in CGXII minimal medium (pH 6.5) supplemented with 40 g L^{-1} glucose, 1 mM IPTG and 1.04 mM $FeSO_4$. Supernatants were analysed after 72 h (A) and 48 h (B). Values and error bars represent means and standard deviations (n = 3 cultivations).

cadaverine is a major by-product of 3-HC production is commensurate with the inability of KDO_{Fj} to hydroxylate cadaverine to 3-HC. Identification and use of KDO enzymes hydroxylating also cadaverine may help increas 3-HC production.

Hydroxylation by KDOs is associated with loss of carbon as carbon dioxide, which negatively impacts the carbon efficiency of the process in addition to the loss of carbon dioxide by decarboxylation of 4-HL. The use of enzymes, which are capable to perform C-H-hydroxylation without using 2-OG as cosubstrate is desirable, such as monooxygenases (EC 1.14.16), which use pteridines as cosubstrates to regiospecifically hydroxylate aromatic amino acids (Pey et al., 2006; Zhang et al., 2006, 2006, p. 2). Comparable to the KDOs, they are highly specific for their natural and closely related substrates. The tyrosine 3-monooxygenase from *Homo sapiens* can accept next to tyrosine with lower efficiency structurally related amino acids like phenylalanine and tryptophan (Roberts and Fitzpatrick, 2013). Alternatively, NAD(P)H/$FADH_2$-dependent monooxygenases (EC 1.14.13.) use reduction equivalents as cofactors, and form the *N*-hydroxylated product and water. One example is the L-lysine N6-monooxygenase, which converts lysine to N6-hydroxy-L-lysine. (Dick et al., 2002).

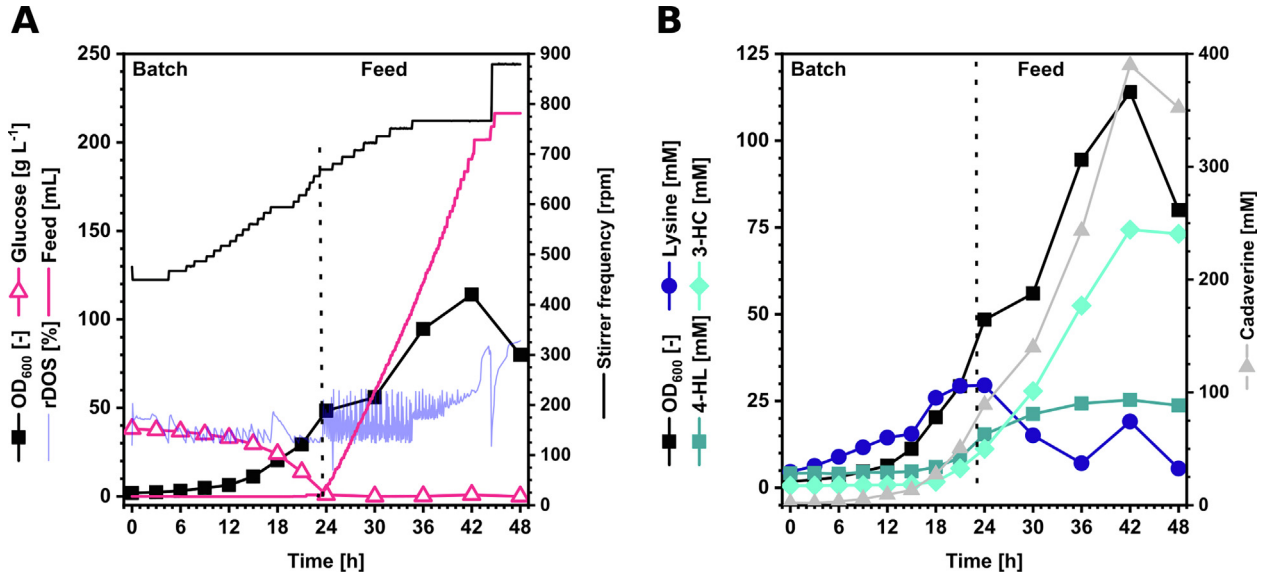

Fig. 7. 3-HC production by *C. glutamicum* HCad1 operated in fed-batch mode. HCad1 was cultivated in 1 L CGXII minimal medium in fed-batch mode over 48 h, containing 40 g L^{-1} glucose from the batch medium and 95 g L^{-1} glucose from the feeding solution. (**A**) OD_{600} is shown in black squares, glucose concentration (g L^{-1}) is plotted as pink empty triangles, feed solution (mL) is depicted as pink line, the relative dissolved oxygen saturation (rDOS, %) is indicated in light blue and the stirrer frequency (rpm) is shown as black line. (**B**) 3-HC production is indicated in light blue diamonds (mM), OD_{600} is shown in black squares, lysine in dark blue circles (mM), 4-HL in turquoise squares (mM), and cadaverine concentration (mM) in grey triangles. Cultivation was performed at 30 °C, 0.75 vvm and a constant pH 6.5 regulated with 10 % (*v/v*) H_3PO_4 and 25% (*w/v*) ammonia. The pO2 was kept above 30% by a stepwise increase in stirrer rate. An overpressure of 0.5 bar was applied. 0.6 mL L^{-1} of antifoam agent AF204 (Sigma Aldrich, Taufkirchen, Germany) was added to the medium manually before inoculation. Plasmid-based overexpression of *ldcC* was induced after 24 h with 1 mM IPTG. (For interpretation of the references to colour in this figure legend, the reader is referred to the web version of this article.)

KDO enzymes require iron and increasing the iron concentration in the growth medium improved production of hydroxylated glutarate involving CsiD from *P. putida* (Prell et al., 2021) and, as described here, of hydroxylated lysine involving KDO_{Fj} (Fig. 2). Increasing the medium iron concentration may positively affect iron cluster containing TCA cycle enzymes such as aconitase or succinate dehydrogenase although the standard iron concentration in CGXII medium is sufficient for growth and does not trigger stress response in *C. glutamicum* (Wennerhold et al., 2005). KDO enzymes depend on 2-OG as cosubstrate. However, increasing provision of 2-OG is difficult since it is part of the TCA cycle. Replenishing the TCA cycle by anaplerotic reactions could help to provide more 2-OG for the KDO enzyme as has been shown for increased supply of oxaloacetate for lysine production and 2-OG for glutamate production by *C. glutamicum* (Peters-Wendisch et al., 2001).

Transport engineering, e.g., by overexpression of the endogenous *thrE* gene improved threonine production in *C. glutamicum* (Simic et al., 2002), while overexpression of *lysE* increased arginine production in *Corynebacterium crenatum* (Xu et al., 2013). It is known that CgmA is involved in cadaverine export and *cgmA* can be overexpressed for improved cadaverine production (Kind et al., 2011; Nguyen et al., 2015a). As it was demonstrated that deletion of *cgmA* also abolished 3-HC accumulation (Fig. 6B), CgmA likely functions as export system for 3-HC. In the case of 4-HL and lysine, indirect evidence may indicate that LysE is involved in 4-HL export. In the absence of LysE, high intracellular lysine concentrations (e.g. due to dipeptide feeding or lysine overproduction) drastically perturb growth of C. *glutamicum* (Vrljic et al., 1996), which can be avoided by conversion of lysine, e.g., to pipecolic acid, which is exported independently of LysE (Pérez-García et al., 2017). Conversion of lysine to 4-HL did not abolish the growth perturbation observed in the 4-HL producer HLys2 that lacks LysE (Table 6). Overexpression of *lysE* may lead to loss of lysine as precursor of 4-HL, thus, decreasing 4-HL production. As alternative, lysine re-uptake into the cell by overexpression of the gene coding for the lysine importer LysI (Seep-Feldhaus et al., 1991) may improve 4-HL production under the hitherto unknown condition that LysI does not accept 4-HL.

Different metabolic engineering strategies were applied to increase provision of 2-OG as cosubstrate of KDOs (Jing et al., 2021). Smirnov et al. (2010) blocked the TCA cycle in *E. coli* by several deletions to avoid conversion from 2-OG to succinate and to couple KDO activity, which provides succinate from 2-OG besides hydroxylating the primary substrate (in this case isoleucine dioxygenase was used) (Smirnov et al., 2010). In a comparable approach, a tunable circuit for dynamic attenuation of ODHC activity was adopted to enhance the flux towards 2-OG and consequently trans-4-hydroxyproline production (Long et al., 2020). In this study, addition of extracellular 2-OG decreased the lysine titer but did not increase the 4-HL titer. Increasing repression of ODHC by $OdhI^{T14A}$ led to 4.4-fold more accumulation of 2-OG in Lys5, but at the expense of lysine production as its biosynthesis is derived from oxalacetate, an intermediate of the TCA cycle (Georgi et al., 2005; Schrumpf et al., 1991). Moreover, glutamate accumulated, while 4-HL was not improved. Possibly, withdrawal of oxaloacetate for lysine production is more important than provision of 2-OG for KDO.

Activities of KDOs respond to the intracellular pH. Lowering the external pH of the cultivation media to 6.5 resulted in increased production of lysine and 4-HL, while perturbing growth. *C. glutamicum* maintains pH homeostasis in a medium pH range from 6.0 to 9.0 (Täuber et al., 2021). Pleiotropic effects of changing the medium pH (i.a., iron starvation, protein folding, and stabilization) (Martín-Galiano et al., 2005) preclude interpretation of these effects of 4-HL production.

The inducible and constitutive lysine decarboxylases, CadA (Kanjee et al., 2011; Sabo et al., 1974) and LdcC (Yamamoto et al., 1997) from *E. coli* were tested with regard to decarboxylation of 4- and 5-hydroxylysine as alternative substrates. CadA is highly efficient, but the enzyme has its optimum at acidic pH (pH 5.0–6.0) and is rapidly inactivated at higher pH (>8.0) (Lemonnier and Lane, 1998) and inhibited at high concentrations of lysine (Kim et al., 2015) or cadaverine (Sabo et al., 1974). Therefore, for *in vivo* production LdcC proved to be superior as it exhibits a broader pH range (Kind et al., 2010) and is hardly inhibited by its substrate (Shin et al., 2018). The third decarboxylase DC_{Fj} tested in this study was investigated before as the genes coding for the lysine-4-hydroxylase KDO_{Fj} (Fjoh_3169) and the PLP-dependent decarboxylase (Fjoh_3171) were found co-localized in the genome of *Flavobacterium johnsoniae* and as it decarboxylated 4-HL to 3-HC (Baud et al., 2017). While the main advantage of DC_{Fj} is its substrate preference for 4-HL (rather than lysine), its activity *in vivo* was low. Further metabolic engineering for optimised expression including optimisation of the ribosome binding site, using different expression systems, and adaption of the codon usage to *C. glutamicum,* as the sequence is rather TA-rich (63 %), might be the key to making use of this substrate preference.

The process was successfully scaled up and the titer increased 7-fold to 74 mM 3-HC. As KDOs are oxygen-dependent enzymes (Martinez and Hausinger, 2015), the process may have benefitted from better aeration. It was shown before, that the aeration rate of the process had a major effect on the production of L-2-hydroxyglutarate by *C. glutamicum* using the KDO glutarate dioxygenase CsiD (Prell et al., 2021). It remains to be studied if 3-HC can be separated from cadaverine efficiently in downstream processing. This and other challenges remain to be solved before the proof-of-concept of 3-HC production can be transferred to industrial application.

Funding

This research was funded in part by the European Regional Development Fund (ERDF) and the Ministry of Economic Affairs, Innovation, Digitalization and Energy of the State of North Rhine-Westphalia by grant “Cluster Industrial Biotechnology (CLIB) Kompetenzzentrum Biotechnologie (CKB)” (34.EFRE-0300095/1703FI04). Florian Meyer was funded by BMBF (KaroTec; grant number: 03VP09460). Fernando Pérez-García was funded by the Norwegian University of Science and Technology (NTNU). Support for the Article Processing Charge by the Deutsche Forschungsgemeinschaft and the Open Access Publication Fund of Bielefeld University is acknowledged. The funding bodies had no role in the design of the study or the collection, analysis, or interpretation of data or in writing the manuscript.

CRediT authorship contribution statement

Carina Prell: Conceptualization, Methodology, Formal analysis, Investigation, Visualization, Writing – original draft, Writing – review & editing. **Sophie-Ann Vonderbank:** Investigation. **Florian Meyer:** Methodology, Investigation, Writing – review & editing. **Fernando Pérez-García:** Conceptualization, Writing – review & editing. **Volker F. Wendisch:** Conceptualization, Supervision, Funding acquisition, Project administration, Writing – review & editing.

Declaration of Competing Interest

The authors declare that they have no known competing financial interests or personal relationships that could have appeared to influence the work reported in this paper.

Acknowledgments

We thank Dr. Joe Risse and Dipl.-Ing. Thomas Schäffer from Fermentation Technology, Technical Faculty & CeBiTec, University of

Bielefeld, for technical assistance and kind advice. Additionally, we thank Daniel Krüger and Arno Krieger for technical assistance.

Appendix

Figure S1: Overlayed HPLC chromatograms of enzymatic KDO assays with crude extracts from *C. glutamicum*. Figure S1: Overlayed HPLC chromatograms of enzymatic DC assays with crude extracts from *C. glutamicum*. Table S1. Retention times and structures for different substrates and products derived from the enzymatic assays.

Ethical approval

This article does not contain any studies with human participants or animal experiments performed by any of the authors.

Appendix A. Supplementary material

Supplementary data to this article can be found online at https://doi.org/10.1016/j.crbiot.2021.12.004.

References

Amatuni, A., Renata, H., 2019. Identification of a lysine 4-hydroxylase from the glidobactin biosynthesis and evaluation of its biocatalytic potential. Org. Biomol. Chem. 17 (7), 1736–1739. https://doi.org/10.1039/C8OB02054J.

Bastard, K., Isabet, T., Stura, E.A., Legrand, P., Zaparucha, A., 2018. Structural studies based on two lysine dioxygenases with distinct regioselectivity brings insights into enzyme specificity within the clavaminate synthase-like family. Sci. Rep. 8, 16587. https://doi.org/10.1038/s41598-018-34795-9.

Baud, D., Peruch, O., Saaidi, P.-L., Fossey, A., Mariage, A., Petit, J.-L., Salanoubat, M., Vergne-Vaxelaire, C., de Berardinis, V., Zaparucha, A., 2017. Biocatalytic approaches towards the synthesis of chiral amino alcohols from lysine: cascade reactions combining alpha-keto acid oxygenase hydroxylation with pyridoxal phosphate- dependent decarboxylation. Adv. Synth. Catal. 359 (9), 1563–1569. https://doi.org/10.1002/adsc.201600934.

Baud, D., Saaidi, P.-L., Monfleur, A., Harari, M., Cuccaro, J., Fossey, A., Besnard, M., Debard, A., Mariage, A., Pellouin, V., Petit, J.-L., Salanoubat, M., Weissenbach, J., de Berardinis, V., Zaparucha, A., 2014. Synthesis of mono- and dihydroxylated amino acids with new α-ketoglutarate-dependent dioxygenases: biocatalytic oxidation of C-H bonds. Chem. Cat. Chem. 6 (10), 3012–3017. https://doi.org/10.1002/cctc.201402498.

Bertani, G., 1951. Studies on lysogenesis. I. The mode of phage liberation by lysogenic *Escherichia coli*. J. Bacteriol. 62 (3), 293–300. https://doi.org/10.1128/jb.62.3.293-300.1951.

Bornscheuer, U.T., Huisman, G.W., Kazlauskas, R.J., Lutz, S., Moore, J.C., Robins, K., 2012. Engineering the third wave of biocatalysis. Nature 485 (7397), 185–194. https://doi.org/10.1038/nature11117.

Burgardt, A., Prell, C., Wendisch, V.F., 2021. Utilization of a wheat sidestream for 5-aminovalerate production in *Corynebacterium glutamicum*. Front. Bioeng. Biotechnol. 9, 772. https://doi.org/10.3389/fbioe.2021.732271.

Cheng, J., Chen, P., Song, A., Wang, D., Wang, Q., 2018. Expanding lysine industry: industrial biomanufacturing of lysine and its derivatives. J. Ind. Microbiol. Biotechnol. 45, 719–734. https://doi.org/10.1007/s10295-018-2030-8.

Dick, S., Siemann, S., Frey, H.E., Lepock, J.R., Viswanatha, T., 2002. Recombinant lysine:N6-hydroxylase: effect of cysteine→alanine replacements on structural integrity and catalytic competence. BBA 1594 (2), 219–233. https://doi.org/10.1016/S0167-4838(01)00305-3.

Dunham, N.P., Chang, W.-C., Mitchell, A.J., Martinie, R.J., Zhang, B.o., Bergman, J.A., Rajakovich, L.J., Wang, B.o., Silakov, A., Krebs, C., Boal, A.K., Bollinger, J.M., 2018. Two distinct mechanisms for C-C desaturation by iron(II)- and 2-(oxo)glutarate-dependent oxygenases: importance of α-heteroatom assistance. J. Am. Chem. Soc. 140 (23), 7116–7126. https://doi.org/10.1021/jacs.8b0193310.1021/jacs.8b01933.s001.

Eggeling, L., Bott, M. (Eds.), 2004. Handbook of *Corynebacterium glutamicum*. CRC Press LLC, Boca Raton, FL. Doi. https://doi.org/10.1007/s10750-004-4543-6.

Eikmanns, B.J., Thum-Schmitz, N., Eggeling, L., Ludtke, K.-U., Sahm, H., 1994. Nucleotide sequence, expression and transcriptional analysis of the *Corynebacterium glutamicum gltA* gene encoding citrate synthase. Microbiology 140 (8), 1817–1828.

Georgi, T., Rittmann, D., Wendisch, V.F., 2005. Lysine and glutamate production by *Corynebacterium glutamicum* on glucose, fructose and sucrose: roles of malic enzyme and fructose-1,6-bisphosphatase. Metab. Eng. 7 (4), 291–301. https://doi.org/10.1016/j.ymben.2005.05.001.

Gibson, D.G., Young, L., Chuang, R.-Y., Venter, J.C., Hutchison, C.A., Smith, H.O., 2009. Enzymatic assembly of DNA molecules up to several hundred kilobases. Nat. Methods 6 (5), 343–345. https://doi.org/10.1038/nmeth.1318.

Goering, A.W., McClure, R.A., Doroghazi, J.R., Albright, J.C., Haverland, N.A., Zhang, Y., Ju, K.-S., Thomson, R.J., Metcalf, W.W., Kelleher, N.L., 2016. Metabologenomics: correlation of microbial gene clusters with metabolites drives discovery of a nonribosomal peptide with an unusual amino acid monomer. ACS Cent. Sci. 2 (2), 99–108. https://doi.org/10.1021/acscentsci.5b00331.

Gómez, R.V., Varela, O., 2007. Synthesis of regioisomeric, stereoregular AABB-type polyamides from chiral diamines and diacids derived from natural amino acids. Tetrahedron Asymmetry 18 (18), 2190–2196. https://doi.org/10.1016/j.tetasy.2007.09.010.

Gunji, Y., Yasueda, H., 2006. Enhancement of L-lysine production in methylotroph *Methylophilus methylotrophus* by introducing a mutant LysE exporter. J. Biotechnol. 127 (1), 1–13. https://doi.org/10.1016/j.jbiotec.2006.06.003.

Hanahan, D., 1985. Techniques for transformation of *E. coli*. DNA cloning: A Practical Approach 1, 109–135.

Hara, R., Yamagata, K., Miyake, R., Kawabata, H., Uehara, H., Kino, K., 2017. Discovery of lysine hydroxylases in the clavaminic acid synthase-like superfamily for efficient hydroxylysine bioproduction. Appl. Environ. Microbiol. 83 (e00693–17), e00693–17. https://doi.org/10.1128/AEM.00693-17.

Hausinger, R.P., 2004. Fe(II)/α-ketoglutarate-dependent hydroxylases and related enzymes. Crit. Rev. Biochem. Mol. Biol. 39 (1), 21–68. https://doi.org/10.1080/10409230490440541.

Henke, N.A., Krahn, I., Wendisch, V.F., 2021. Improved plasmid-based inducible and constitutive gene expression in *Corynebacterium glutamicum*. Microorganisms 9, 204. https://doi.org/10.3390/microorganisms9010204.

Herbert, K.R., Williams, G.M., Cooper, G.J.S., Brimble, M.A., 2012. Synthesis of glycosylated 5-hydroxylysine, an important amino acid present in collagen-like proteins such as adiponectin. Org. Biomol. Chem. 10 (6), 1137. https://doi.org/10.1039/c1ob06394d.

Jakob, K., Satorhelyi, P., Lange, C., Wendisch, V.F., Silakowski, B., Scherer, S., Neuhaus, K., 2007. Gene expression analysis of *Corynebacterium glutamicum* subjected to long-term lactic acid adaptation. J. Bacteriol. 189 (15), 5582–5590. https://doi.org/10.1128/JB.00082-07.

Jing, X., Liu, H., Nie, Y., Xu, Y., 2021. Advances in Fe(II)/2-ketoglutarate-dependent dioxygenase-mediated C-H bond oxidation for regioselective and stereoselective hydroxyl amino acid synthesis: from structural insights into practical applications. Syst. Microbiol. and Biomanuf. 1 (3), 275–290. https://doi.org/10.1007/s43393-021-00025-z.

Jorge, J.M.P., Pérez-García, F., Wendisch, V.F., 2017. A new metabolic route for the fermentative production of 5-aminovalerate from glucose and alternative carbon sources. Biores. Technol. 245, 1701–1709. https://doi.org/10.1016/j.biortech.2017.04.108.

Kakwere, H., Perrier, S., 2011. Design of complex polymeric architectures and nanostructured materials/hybrids by living radical polymerization of hydroxylated monomers. Polym. Chem. 2 (2), 270–288. https://doi.org/10.1039/C0PY00160K.

Kanjee, U., Gutsche, I., Alexopoulos, E., Zhao, B., El Bakkouri, M., Thibault, G., Liu, K., Ramachandran, S., Snider, J., Pai, E.F., Houry, W.A., 2011. Linkage between the bacterial acid stress and stringent responses: the structure of the inducible lysine decarboxylase: Linkage between the bacterial acid stress and stringent responses. The EMBO Journal 30, 931–944. https://doi.org/10.1038/emboj.2011.5.

Kim, Barıtugo, Oh, Kang, Jung, Jang, Song, Kim, Lee, Hwang, Park, Park, Joo, 2019. High-Level Conversion of l-lysine into Cadaverine by *Escherichia coli* Whole Cell Biocatalyst Expressing *Hafnia alvei* l-lysine Decarboxylase. Polymers 11, 1184. Doi: 10.3390/polym11071184.

Kim, H.J., Kim, Y.H., Shin, J.-H., Bhatia, S.K., Sathiyanarayanan, G., Seo, H.-M., Choi, K. Y., Yang, Y.-H., Park, K., 2015. Optimization of direct lysine decarboxylase biotransformation for cadaverine production with whole-cell biocatalysts at high lysine concentration. J. Microbiol. Biotechnol. 25 (7), 1108–1113. https://doi.org/10.4014/jmb.1412.12052.

Kim, H.T., Barıtugo, K.-A., Oh, Y.H., Hyun, S.M., Khang, T.U., Kang, K.H., Jung, S.H., Song, B.K., Park, K., Kim, I.-K., Lee, M.O., Kam, Y., Hwang, Y.T., Park, S.J., Joo, J.C., 2018. Metabolic engineering of *Corynebacterium glutamicum* for the high-level production of cadaverine that can be used for the synthesis of biopolyamide 510. ACS Sustain. Chem. Eng. 6 (4), 5296–5305. https://doi.org/10.1021/acssuschemeng.8b0000910.1021/acssuschemeng.8b00009.s001.

Kind, S., Jeong, W.K., Schröder, H., Zelder, O., Wittmann, C., 2010. Identification and elimination of the competing *N* -acetyldiaminopentane pathway for improved production of diaminopentane by *Corynebacterium glutamicum*. Appl. Microbiol. Biotechnol. 76 (15), 5175–5180. https://doi.org/10.1128/AEM.00834-10.

Kind, S., Kreye, S., Wittmann, C., 2011. Metabolic engineering of cellular transport for overproduction of the platform chemical 1,5-diaminopentane in *Corynebacterium glutamicum*. Metab. Eng. 13 (5), 617–627. https://doi.org/10.1016/j.ymben.2011.07.006.

Koontz, L., 2014. TCA Precipitation, in: Methods in Enzymology. Academic Press, Cambrige, MA, pp. 3–10. Doi: 10.1016/B978-0-12-420119-4.00001-X.

Krämer, A.B., R., 2002. Bacterial amino acid transport proteins: occurrence, functions, and significance for biotechnological applications. Appl. Microbiol. Biotechnol. 58, 265–274. Doi: 10.1007/s00253-001-0869-4.

Lamarre, D., Croteau, G., Wardrop, E., Bourgon, L., Thibeault, D., Clouette, C., Vaillancourt, M., Cohen, E., Pargellis, C., Yoakim, C., Anderson, P.C., 1997. Antiviral properties of palinavir, a potent inhibitor of the human immunodeficiency virus type 1 protease. Antimicrob. Agents Chemother. 41 (5), 965–971. https://doi.org/10.1128/AAC.41.5.965.

Lampe, J.W., Hughes, P.F., Biggers, C.K., Smith, S.H., Hu, H., 1996. Total Synthesis of (−)- and (+)-Balanol [1]. J. Org. Chem. 61 (14), 4572–4581. https://doi.org/10.1021/jo952280k.

Lemonnier, M., Lane, D., 1998. Expression of the second lysine decarboxylase gene of *Escherichia coli*. Microbiology 144, 751–760. https://doi.org/10.1099/00221287-144-3-751.

Leßmeier, L., Pfeifenschneider, J., Carnicer, M., Heux, S., Portais, J.-C., Wendisch, V.F., 2015. Production of carbon-13-labeled cadaverine by engineered *Corynebacterium glutamicum* using carbon-13-labeled methanol as co-substrate. Appl. Microbiol. Biotechnol. 99 (23), 10163–10176. https://doi.org/10.1007/s00253-015-6906-5.

Long, M., Xu, M., Ma, Z., Pan, X., You, J., Hu, M., Shao, Y., Yang, T., Zhang, X., Rao, Z., 2020. Significantly enhancing production of *trans* -4-hydroxy-l-proline by integrated system engineering in *Escherichia coli*. Sci. Adv. 6, eaba2383. https://doi.org/10.1126/sciadv.aba2383.

Lubitz, D., Jorge, J.M.P., Pérez-García, F., Taniguchi, H., Wendisch, V.F., 2016. Roles of export genes *cgmA* and *lysE* for the production of L-arginine and L-citrulline by *Corynebacterium glutamicum*. Appl. Microbio.l Biotechnol. 100 (19), 8465–8474. https://doi.org/10.1007/s00253-016-7695-1.

Martinez, S., Hausinger, R.P., 2015. Catalytic mechanisms of Fe(II)- and 2-oxoglutarate-dependent oxygenases. J. Biol. Chem. 290 (34), 20702–20711. https://doi.org/10.1074/jbc.R115.648691.

Martín-Galiano, A.J., Overweg, K., Ferrándiz, M.J., Reuter, M., Wells, J.M., de la Campa, A.G., 2005. Transcriptional analysis of the acid tolerance response in *Streptococcus pneumoniae*. Microbiology 151, 3935–3946. https://doi.org/10.1099/mic.0.28238-0.

Mimitsuka, T., Sawai, H., Hatsu, M., Yamada, K., 2007. Metabolic engineering of *Corynebacterium glutamicum* for cadaverine fermentation. Biosci. Biotechnol. Biochem. 71 (9), 2130–2135. https://doi.org/10.1271/bbb.60699.

Mitchell, A.J., Dunham, N.P., Martinie, R.J., Bergman, J.A., Pollock, C.J., Hu, K., Allen, B.D., Chang, W.-C., Silakov, A., Bollinger, J.M., Krebs, C., Boal, A.K., 2017. Visualizing the reaction cycle in an Iron(II)- and 2-(Oxo)-glutarate-dependent hydroxylase. J. Am. Chem. Soc. 139 (39), 13830–13836. https://doi.org/10.1021/jacs.7b0737410.1021/jacs.7b07374.s001.

Nguyen, A.Q.D., Schneider, J., Reddy, G.K., Wendisch, V.F., 2015a. Fermentative production of the diamine putrescine: system metabolic engineering of *Corynebacterium glutamicum*. Metabolites 5, 211–231. https://doi.org/10.3390/metabo5020211.

Nguyen, A.Q.D., Schneider, J., Wendisch, V.F., 2015b. Elimination of polyamine *N*-acetylation and regulatory engineering improved putrescine production by *Corynebacterium glutamicum*. J. Biotechnol. Mol. Biotechnol.: Enzymes Metabol. Eng. Microbes Superior Sustain. Products Processes 201, 75–85. https://doi.org/10.1016/j.jbiotec.2014.10.035.

Oh, Y.H., Choi, J.W., Kim, E.Y., Song, B.K., Jeong, K.J., Park, K., Kim, I.-K., Woo, H.M., Lee, S.H., Park, S.J., 2015. Construction of synthetic promoter-based expression cassettes for the production of cadaverine in recombinant *Corynebacterium glutamicum*. Appl. Biochem. Biotechnol. 176 (7), 2065–2075. https://doi.org/10.1007/s12010-015-1701-4.

Orgueira, H.A., Erra-Balsells, R., Nonami, H., Varela, O., 2001. Synthesis of chiral polyhydroxy polyamides having chains of defined regio and stereoregularity. Macromolecules 34, 687–695. https://doi.org/10.1021/ma000016+.

Pérez-García, F., Jorge, J.M.P., Dreyszas, A., Risse, J.M., Wendisch, V.F., 2018. Efficient production of the dicarboxylic acid glutarate by *Corynebacterium glutamicum* via a novel synthetic pathway. Front. Microbiol. 9, 2589. https://doi.org/10.3389/fmicb.2018.02589.

Pérez-García, F., Max Risse, J., Friehs, K., Wendisch, V.F., 2017. Fermentative production of L-pipecolic acid from glucose and alternative carbon sources. Biotechnol. J. 12 (7), 1600646. https://doi.org/10.1002/biot.v12.710.1002/biot.201600646.

Pérez-García, F., Wendisch, V.F., 2018. Transport and metabolic engineering of the cell factory *Corynebacterium glutamicum*. FEMS Microbiol. Lett. 365, fny166. https://doi.org/10.1093/femsle/fny166.

Peters, C., Buller, R., 2019. Industrial application of 2-oxoglutarate-dependent oxygenases. Catalysts 9, 221. https://doi.org/10.3390/catal9030221.

Peters-Wendisch, P.G., Schiel, B., Wendisch, V.F., Katsoulidis, E., Möckel, B., Sahm, H., Eikmanns, B.J., 2001. Pyruvate carboxylase is a major bottleneck for glutamate and lysine production by *Corynebacterium glutamicum*. J. Mol. Microbiol. Biotechnol. 3, 295–300.

Pey, A.L., Martinez, A., Charubala, R., Maitland, D.J., Teigen, K., Calvo, A., Pfleiderer, W., Wood, J.M., Schallreuter, K.U., Pey, A.L., Martinez, A., Charubala, R., Maitland, D.J., Teigen, K., Calvo, A., Pfleiderer, W., Wood, J.M., Schallreuter, K.U., 2006. Specific interaction of the diastereomers 7(R)- and 7(S)-tetrahydrobiopterin with phenylalanine hydroxylase: implications for understanding primapterinuria and vitiligo. FASEB j. 20 (12), 2130–2132. https://doi.org/10.1096/fj.06-5835fje.

Prell, C., Burgardt, A., Meyer, F., Wendisch, V.F., 2021. Fermentative production of L-2-hydroxyglutarate by engineered *Corynebacterium glutamicum* via pathway extension of L-lysine biosynthesis. Front. Bioeng. Biotechnol. 8,. https://doi.org/10.3389/fbioe.2020.630476 630476.

Ren, X., Fasan, R., 2021. Engineered and artificial metalloenzymes for selective C-H functionalization. Curr. Opin. Green Sustain. Chem. 31, 100494. https://doi.org/10.1016/j.cogsc.2021.100494.

Roberts, K.M., Fitzpatrick, P.F., 2013. Mechanisms of tryptophan and tyrosine hydroxylase. IUBMB Life 65 (4), 350–357. https://doi.org/10.1002/iub.1144.

Sabo, D.L., Boeker, E.A., Byers, B., Waron, H., Fischer, E.H., 1974. Purification and physical properties of inducible *Escherichia coli* lysine decarboxylase. J. Biochem. 13 (4), 662–670. https://doi.org/10.1021/bi00701a005.

Salis, H.M., 2011. Chapter two - The Ribosome Binding Site Calculator. In: Voigt, C. (Ed.), Methods in Enzymology, Synthetic Biology, Part B. Academic Press, Cambrige, MA, pp. 19–42. https://doi.org/10.1016/B978-0-12-385120-8.00002-4.

Schneider, J., Niermann, K., Wendisch, V.F., 2011. Production of the amino acids L-glutamate, L-lysine, L-ornithine and L-arginine from arabinose by recombinant *Corynebacterium glutamicum*. J. Biotechnol. 154 (2–3), 191–198. https://doi.org/10.1016/j.jbiotec.2010.07.009.

Schneider, J., Wendisch, V.F., 2010. Putrescine production by engineered *Corynebacterium glutamicum*. Appl. Microbiol. Biotechnol. 88 (4), 859–868. https://doi.org/10.1007/s00253-010-2778-x.

Schrumpf, B., Schwarzer, A., Kalinowski, J., Pühler, A., Eggeling, L., Sahm, H., 1991. A functionally split pathway for lysine synthesis in *Corynebacterium glutamicum*. J. Bacteriol. 173, 4510–4516. https://doi.org/10.1128/jb.173.14.4510-4516.1991.

Seep-Feldhaus, A.H., Kalinowski, J., Pühler, A., 1991. Molecular analysis of the *Corynebacterium glutamicum lysI* gene involved in lysine uptake. Mol. Microbiol. 5, 2995–3005. https://doi.org/10.1111/j.1365-2958.1991.tb01859.x.

Sheldon, R.A., Woodley, J.M., 2018. Role of biocatalysis in sustainable chemistry. Chem. Rev. 118 (2), 801–838. https://doi.org/10.1021/acs.chemrev.7b00203.

Shin, J., Joo, J.C., Lee, E., Hyun, S.M., Kim, H.J., Park, S.J., Yang, Y.-H., Park, K., 2018. Characterization of a whole-cell biotransformation using a constitutive lysine decarboxylase from *Escherichia coli* for the high-level production of cadaverine from industrial grade L-lysine. Appl. Biochem. Biotechnol. 185 (4), 909–924. https://doi.org/10.1007/s12010-018-2696-4.

Simic, P., Willuhn, J., Sahm, H., Eggeling, L., 2002. Identification of *glyA* (encoding serine hydroxymethyltransferase) and its use together with the exporter ThrE to increase L -threonine accumulation by *Corynebacterium glutamicum*. Appl. Environ. Microbiol. 68, 3321–3327. https://doi.org/10.1128/AEM.68.7.3321-3327.2002.

Simon, R., Priefer, U., Pühler, A., 1983. A broad host range mobilization system for in vivo genetic engineering: transposon mutagenesis in Gram negative bacteria. Bio/Technology 1 (9), 784–791. https://doi.org/10.1038/nbt1183-784.

Smirnov, S.V., Kodera, T., Samsonova, N.N., Kotlyarova, V.A., Rushkevich, N.Y., Kivero, A.D., Sokolov, P.M., Hibi, M., Ogawa, J., Shimizu, S., 2010. Metabolic engineering of *Escherichia coli* to produce (2S, 3R, 4S)-4-hydroxyisoleucine. Appl. Microbiol. Biotechnol. 88 (3), 719–726. https://doi.org/10.1007/s00253-010-2772-3.

Smith, W.G., Gilboe, D.P., Henderson, L.M., 1965. Incorporation of hydroxylysine into the cell wall and a cell-wall precursor in *Staphylococcus aureus*. J. Bacteriol. 89 (1), 136–140.

Stansen, C., Uy, D., Delaunay, S., Eggeling, L., Goergen, J.-L., Wendisch, V.F., 2005. Characterization of a *Corynebacterium glutamicum* lactate utilization operon induced during temperature-triggered glutamate production. Appl. Environ. Microbiol. 71 (10), 5920–5928. https://doi.org/10.1128/AEM.71.10.5920-5928.2005.

Strieker, M., Kopp, F., Mahlert, C., Essen, L.-O., Marahiel, M.A., 2007. Mechanistic and structural basis of stereospecific Cβ-hydroxylation in calcium-dependent antibiotic, a daptomycin-type lipopeptide. ACS Chem. Biol. 2 (3), 187–196. https://doi.org/10.1021/cb700012y10.1021/cb700012y.s001.

Sun, H., Zhang, H., Ang, E.L., Zhao, H., 2018. Biocatalysis for the synthesis of pharmaceuticals and pharmaceutical intermediates. Bioorg. Med. Chem. 26 (7), 1275–1284. https://doi.org/10.1016/j.bmc.2017.06.043.

Tateno, T., Okada, Y., Tsuchidate, T., Tanaka, T., Fukuda, H., Kondo, A., 2009. Direct production of cadaverine from soluble starch using *Corynebacterium glutamicum* coexpressing α-amylase and lysine decarboxylase. Appl. Microbiol. Biotechnol. 82 (1), 115–121. https://doi.org/10.1007/s00253-008-1751-4.

Täuber, S., Blöbaum, L., Wendisch, V.F., Grünberger, A., 2021. Growth Response and Recovery of *Corynebacterium glutamicum* Colonies on Single-Cell Level Upon Defined pH Stress Pulses. Front. Microbiol. 12, 711893. Doi: 10.3389/fmicb.2021.711893.

Turpeenniemi-Hujanen, T., Myllylä, R., 1984. Concomitant hydroxylation of proline and lysine residues in collagen using purified enzymes *in vitro*. Biochim. Biophys. Acta. Gen. Subj. 800 (1), 59–65. https://doi.org/10.1016/0304-4165(84)90094-1.

Unthan, S., Baumgart, M., Radek, A., Herbst, M., Siebert, D., Brühl, N., Bartsch, A., Bott, M., Wiechert, W., Marin, K., Hans, S., Krämer, R., Seibold, G., Frunzke, J., Kalinowski, J., Rückert, C., Wendisch, V.F., Noack, S., 2015. Chassis organism from *Corynebacterium glutamicum* – a top-down approach to identify and delete irrelevant gene clusters. Biotechnol. J. 10 (2), 290–301. https://doi.org/10.1002/biot.201400041.

Vrljic, M., Sahm, H., Eggeling, L., 1996. A new type of transporter with a new type of cellular function: l-lysine export from *Corynebacterium glutamicum*. Mol. Microbiol. 22, 815–826. https://doi.org/10.1046/j.1365-2958.1996.01527.x.

Wan, J.-P., Gan, L.u., Liu, Y., 2017. Transition metal-catalyzed C-H bond functionalization in multicomponent reactions: a tool toward molecular diversity. Org. Biomol. Chem. 15 (43), 9031–9043. https://doi.org/10.1039/C7OB02011B.

Wang, F., Zhu, M., Song, Z., Li, C., Wang, Y., Zhu, Z., Sun, D., Lu, F., Qin, H.-M., 2020. Reshaping the binding pocket of lysine hydroxylase for enhanced activity. ACS Catal. 10 (23), 13946–13956. https://doi.org/10.1021/acscatal.0c0384110.1021/acscatal.0c03841.s001.

Wennerhold, J., Krug, A., Bott, M., 2005. The AraC-type regulator RipA represses aconitase and other iron proteins from *Corynebacterium* under iron limitation and is itself repressed by DtxR. J. Biol. Chem. 280 (49), 40500–40508. https://doi.org/10.1074/jbc.M508693200.

Wu, L.-F., Meng, S., Tang, G.-L., 2016. Ferrous iron and α-ketoglutarate-dependent dioxygenases in the biosynthesis of microbial natural products. BBA 1864 (5), 453–470. https://doi.org/10.1016/j.bbapap.2016.01.012.

Xu, M., Rao, Z., Yang, J., Dou, W., Xu, Z., 2013. The effect of a LysE exporter overexpression on L-arginine production in *Corynebacterium crenatum*. Curr. Microbiol. 67 (3), 271–278. https://doi.org/10.1007/s00284-013-0358-x.

Yamamoto, Y., Miwa, Y., Miyoshi, K., Furuyama, J.-I., Ohmori, H., 1997. The *Escherichia coli ldcC* gene encodes another lysine decarboxylase, probably a constitutive enzyme. Genes Genet. Syst. 72 (3), 167–172. https://doi.org/10.1266/ggs.72.167.

Yang, P., Yang, W., 2014. Hydroxylation of organic polymer surface: method and application. ACS Appl. Mater. Interfaces 6 (6), 3759–3770. https://doi.org/10.1021/am405857m.

Zhang, C., Li, Y., Ma, J., Liu, Y., He, J., Li, Y., Zhu, F., Meng, J., Zhan, J., Li, Z., Zhao, L., Ma, Q., Fan, X., Xu, Q., Xie, X., Chen, N., 2018a. High production of 4-hydroxyisoleucine in *Corynebacterium glutamicum* by multistep metabolic engineering. Metab. Eng. 49, 287–298. https://doi.org/10.1016/j.ymben.2018.09.008.

Zhang, X., Beaulieu, J.-M., Gainetdinov, R.R., Caron, M.G., 2006. Functional polymorphisms of the brain serotonin synthesizing enzyme tryptophan hydroxylase-2. Cell. Mol. Life Sci. 63, 6. https://doi.org/10.1007/s00018-005-5417-4.

Zhang, X., King-Smith, E., Renata, H., 2018b. Total synthesis of tambromycin by combining chemocatalytic and biocatalytic C−H functionalization. Angew. Chem. Int. Ed. 57 (18), 5037–5041. https://doi.org/10.1002/anie.201801165.